

Glacial lake outburst flood risk assessment of a rapidly expanding glacial lake in the Ladakh region of Western Himalaya, using hydrodynamic modeling

Abid Farooq Rather, Rayees Ahmed, Joshal Kumar Bansal, Rasiq Ahmad Mir, Pervez Ahmed, Ishfaq Hussain Malik & Divyesh Varade

To cite this article: Abid Farooq Rather, Rayees Ahmed, Joshal Kumar Bansal, Rasiq Ahmad Mir, Pervez Ahmed, Ishfaq Hussain Malik & Divyesh Varade (2024) Glacial lake outburst flood risk assessment of a rapidly expanding glacial lake in the Ladakh region of Western Himalaya, using hydrodynamic modeling, *Geomatics, Natural Hazards and Risk*, 15:1, 2413893, DOI: [10.1080/19475705.2024.2413893](https://doi.org/10.1080/19475705.2024.2413893)

To link to this article: <https://doi.org/10.1080/19475705.2024.2413893>



© 2024 The Author(s). Published by Informa UK Limited, trading as Taylor & Francis Group.



Published online: 21 Oct 2024.



Submit your article to this journal [↗](#)



Article views: 693



View related articles [↗](#)



View Crossmark data [↗](#)

Glacial lake outburst flood risk assessment of a rapidly expanding glacial lake in the Ladakh region of Western Himalaya, using hydrodynamic modeling

Abid Farooq Rather^a, Rayees Ahmed^a, Joshal Kumar Bansal^b, Rasiq Ahmad Mir^c, Pervez Ahmed^a, Ishfaq Hussain Malik^d and Divyesh Varade^c

^aDepartment of Geography and Disaster Management, School of Earth and Environmental Sciences, University of Kashmir, Srinagar, India; ^bCenter of Excellence in Disaster Mitigation and Management, Indian Institute of Technology, Roorkee, India; ^cDepartment of Civil Engineering, Indian Institute of Technology Jammu, Jammu, India; ^dSchool of Geography, University of Leeds, Leeds, UK

ABSTRACT

The ongoing trend of warming climate has made Glacial Lake Outburst Floods (GLOFs) a major cryospheric hazard worldwide, especially in the Himalayas. GLOFs in the Himalayan region are mostly caused by moraine-dammed proglacial lakes and ice-dammed lakes. These sporadic disasters have resulted in significant loss of life and property. This study offers a comprehensive analysis of the GLOF hazard potential of a potentially dangerous proglacial lake (PDGL) in the Ladakh region. This research explores the GLOF threat from the lake using multi-criteria analysis and advanced 2D hydrodynamic modeling approaches. The mass balance response of the mother glacier, its flow dynamics, and glacier-lake interactions were examined for the past 22 years. The findings show that over this period, the PDGL has had a notable expansion of 78.7%, accompanied by a significant recession of 13.2% in its feeding glacier. The glacier has witnessed an average thickness loss of ~ 7 m at the rate of 0.32 m a^{-1} during this period. The average, lowest, and maximum depth of the glacier were found to be 30.95, 14.30, and 50.57 m, respectively and the average velocity of the glacier was estimated as 3.38 m a^{-1} . Because of the lake's rapid expansion and steep surrounding slopes, it was classified as a high-hazard lake. The risk to the downstream community was assessed through 2D hydrodynamic modeling using the HEC-RAS tool. The maximum discharge under the worst-case scenario for the piping and overtopping failures was estimated as $3890.99 \text{ m}^3 \text{ s}^{-1}$ and $5111.39 \text{ m}^3 \text{ s}^{-1}$, respectively. The area potentially under the threat of inundation was calculated to be 4.74 and 5.38 km^2 for the moderate and worst-case scenarios respectively. The expected maximum flood velocities range from 18.26 to 23.78 meters, respectively for the moderate and worst-case scenarios. At several locations in the downstream area, routed hydrographs representing the GLOF propagation were generated. The findings show that the flood wave in the worst-case scenario

ARTICLE HISTORY

Received 5 June 2024
Accepted 3 October 2024

KEYWORDS

GLOF; glacial lake expansion; risk assessment; HECRAS, Ladakh region; Western Himalayas; Panikhar, Kargil

CONTACT Rayees Ahmed  rayeesrashid84@gmail.com

© 2024 The Author(s). Published by Informa UK Limited, trading as Taylor & Francis Group. This is an Open Access article distributed under the terms of the Creative Commons Attribution-NonCommercial License (<http://creativecommons.org/licenses/by-nc/4.0/>), which permits unrestricted non-commercial use, distribution, and reproduction in any medium, provided the original work is properly cited. The terms on which this article has been published allow the posting of the Accepted Manuscript in a repository by the author(s) or with their consent.

would arrive at the first settlement in 50 min, with a peak velocity of 12.36 m s^{-1} . The potentially inundated area includes critical infrastructure such as bridges, residential houses, and roads. To mitigate the potential risk associated with this lake, a more detailed and on-site study is highly recommended.

1. Introduction

In most glaciated parts of the world, the effects of climate change have resulted in ongoing glacier recession and the formation of glacial lakes behind recently exposed unstable moraines (Zemp et al. 2009; Bolch et al. 2012; Nie et al. 2017). Mountain settlements in the Himalayas, where numerous such glacial lakes are created, are seriously at risk from glacial lake outburst floods (Clague and Mathews 1973; Ding and Liu 1992; Ahmed 2024). Glacial lake outburst floods (GLOFs) are catastrophic occurrences that take place when a glacial lake, impounded by a glacier or moraine, breaks, releasing a significant amount of water and debris downstream causing flash floods in the downstream area, ruining crops, damaging infrastructure like bridges and hydro-power plants, and resulting in fatalities. The majority of these flood episodes are linked to processes like dam breach creation and subsequent damming moraine failure (Richardson and Reynolds 2000; Emmer and Vilímek 2013; Worni et al. 2014). The possible triggers of a GLOF event may be glacial calving activity at the lake terminus (Zhang et al. 2020), snow or ice avalanches (Schaub et al. 2016), landslides, extreme weather events (Schmidt et al. 2020) like cloudbursts (Bhambri et al. 2016) or seismic activity (Kargel et al. 2016). These events are potent threats whose effects can reach distances of more than 100 km in the downstream region (Richardson and Reynolds 2000).

GLOFs pose a threat to about 15 million people globally and the most prominent high-vulnerability zone is the Himalayan region followed by the Andes (Taylor et al. 2023). Due to the Himalayan terrain's steep slopes and constrained flow pathways, GLOF episodes have typically been described as being particularly catastrophic (Mool 1995; Reynolds 1998; Richardson and Reynolds 2000; Worni et al. 2013). The recent Kedarnath disaster in the Central Himalayas in June 2013, which was brought on by unrelenting rain and subsequent eruption of the Chorabari glacial lake, serves as an illustration of the degree of fatality these occurrences can bring about (Das et al. 2015; Allen et al. 2016). The increased GLOF hazard in the region requires rigorous research initiatives for the identification and monitoring of hazardous glacial lakes in this region. Given that most of the glacial lakes in the Himalayas are inaccessible because of its tough terrain and harsh climate, remote sensing methods are used to monitor these lakes through time and space. Numerous studies have been conducted in the past to evaluate the distribution and GLOF hazard of glacial lakes throughout the world, especially in the Himalaya, which includes countries like Nepal, Tibet, Bhutan, and India (Bajracharya et al. 2007; Bolch et al. 2008; Fujita et al. 2009; Ives et al. 2010; Shrestha et al. 2010; Raj et al. 2013; Rounce et al. 2017; Emmer et al. 2018; Jiang et al. 2018; Nie et al. 2018; Byers et al. 2018; Emmer et al. 2020; Ashraf et al. 2021; Ahmed et al. 2022a, 2022b; Banerjee and Bhuiyan 2023).

The Himalayan region, hence, has been the most well-known case for GLOF disaster risk studies. In the central Himalayas, a GLOF hazard vulnerability study by the International Centre for Integrated Mountain Development (ICIMOD), highlighted some priority sites for GLOF risk mitigation. The study mapped 1,947 glacial lakes using data from the Global Land Ice Measurement from Space (GLIMS) program, of which 835 were deemed dangerous because of their locations upstream of populated areas and major roadways. The study showed that Nepal urgently needs to reduce GLOF danger, especially in the regions downstream of the 835 little glacial lakes (Bajracharya et al. 2007). Rounce et al. (2017) evaluated the risk presented by GLOFs in Nepal using satellite data from 2000 to 2015 and the previous GLOF data. The risk connected to each lake was estimated by combining the hazard and projected downstream effects. The results reported 31 high-risk lakes and 11 very high-risk lakes.

For the Upper Indus River basin, Gupta et al. (2021) conducted an assessment of potentially hazardous glacial lakes identifying 20 and 48 high-risk lakes for two different GLOF scenarios respectively. The evolving status and potential consequences of glacier lakes and the GLOF threat in the Hindu Kush Himalaya region were studied by Ashraf et al. (2021). An overall increase of 26% in the number of glacial lakes was found from 2001 to 2013 and 36 lakes were characterized as potentially dangerous. The increased risk posed by GLOFs in the context of a warming climate is highlighted, along with the necessity for proactive monitoring, risk assessment, and adaptation measures. From an Indian perspective, Jammu and Kashmir has the highest cumulative degree of GLOF hazard, followed by Uttarakhand, Arunachal Pradesh, Sikkim, Himachal Pradesh, and Arunachal Pradesh (Mal et al. 2021). Dubey and Goyal (2020) also placed J&K in second place, only after Sikkim, concerning the GLOF threat. Ahmed et al. (2022) analyzed the GLOF hazard scenario in the Jhelum basin using remote sensing and GIS and identified 21 potentially dangerous and 7 highly hazardous lakes.

Studies focusing on individual glacial lakes have also been conducted in all parts of the Himalayan region. Majeed et al. (2021) reconstructed the 2014 Gya glacial lake outburst flood in Ladakh using the hydrodynamic model HEC-RAS and the results revealed the possible cause of the GLOF to be the piping failure. The study also predicted the possibility of 5 times more severe GLOF in the future from the lake. Mir et al. (2018) evaluated the GLOF risk of Dalung and Padam lakes in the Zaskar Valley using the Mike 11 model. The results declared both the lakes as potentially dangerous and susceptible to GLOFs of significant intensities. Sattar et al. (2021) analyzed the GLOF potential of Lower Barun glacial lake in Sikkim Himalayas and the lake was found to be susceptible to GLOF in case of a strong triggering event. Ahmed et al. (2023) estimated the risk associated with the Gangabal lake in Kashmir Himalayas using the HEC-RAS model. The results indicate that the lake has the potential to generate a peak discharge of 16,601.03 m³/s in the worst-case scenario at the time of a GLOF event. Rawat et al. (2023a) assessed a PDGL in the Satluj River basin in India and reported an areal expansion from 0.11 to 0.26 km² over the past 28 years from 1990 to 2018 and high GLOF risk. Sattar et al. (2019) conducted the moraine breach modeling of the South Lhonak lake in Sikkim and declared the lake to be highly vulnerable to GLOF, owing to its alarming rate of expansion over the

past few decades and a loosely consolidated moraine dam. This very lake witnessed a severe GLOF disaster on October 4, 2023, killing at least 40 people and destroying public infrastructure in its downstream area. Similar studies have been conducted far and wide in the Himalayas that focus on predictive GLOF modeling of hazardous glacial lakes (Emmer and Vilímek 2013; Haemmig et al. 2014; Klimeš et al. 2014; Round et al. 2017; Wang et al. 2018, Sattar et al. 2019; Hussain et al. 2020; Majeed et al. 2021; Sattar et al. 2021; Ahmed et al. 2022; Wang et al. 2022; Gouli et al. 2023; Das et al. 2024; Schmidt et al., 2020) etc.

The present study is one such attempt at understanding the GLOF hazard risk associated with a rapidly expanding moraine-dammed glacial lake in the Ladakh region of the Western Himalayas using multi-criteria decision analysis and 2D GLOF modeling. The identified PDGL is situated above the Panikhar and Pranti villages in the Kargil district of Ladakh. This study focused on the following objectives. (1) Studying the glacier-lake interactions of the Panikhar glacier and glacial lake for the past 22 years (2) Estimating the mass balance, ice thickness, and surface velocity of the Panikhar glacier, (3) Assessing the GLOF hazard level of the lake and associated risk to the downstream community using geospatial analysis and hydrodynamic modeling.

2. Study area

The glacial lake under investigation in this study is situated above the Panikhar and Pranti villages of the Kargil district in the Suru River catchment of the Western Himalayas. This lake is located between $34^{\circ}2'2.154''N$ latitude and $75^{\circ}46'59.172''E$ longitude, 4062 meters above sea level while its mother glacier lies, in close proximity, to its West (Figure 1). The Suru catchment is drained by the Suru River which flows through Kargil district and subsequently joins the Indus as its left bank tributary. The total catchment area is 4408 km^2 and the elevation range is from 2588 masl to 7047 masl. The mother glacier of the lake (GLIMS ID: G075817E34034N) is situated in the southwest of the Suru River catchment at a distance of about 15 kilometers from the well-known Parkachik glacier. The glacial lake or its mother glacier has not been identified with any specific names in previous literature. Because of this, we have given them the names of the village that is closest to them: Panikhar Glacier and Glacial Lake. The Panikhar village is situated about 13 kilometers downstream in the North-East of the glacier-lake complex and is vulnerable to potential GLOF events from the lake.

2.1. Glacial geomorphology

Panikhar glacier is oriented in the West-East direction and the lake is proglacially located close to its snout at its eastern side. The ablation zone of the glacier exhibits a bend towards the northeast according to the local geomorphology. The elevation of the glacial valley ranges from 5500 to 4100 meters above sea level (masl) and the glacial lake is situated at a height of 4100 masl. The contour lines clearly show that the steep slope to the northwest of the glacial lake is prone to landslides and snow

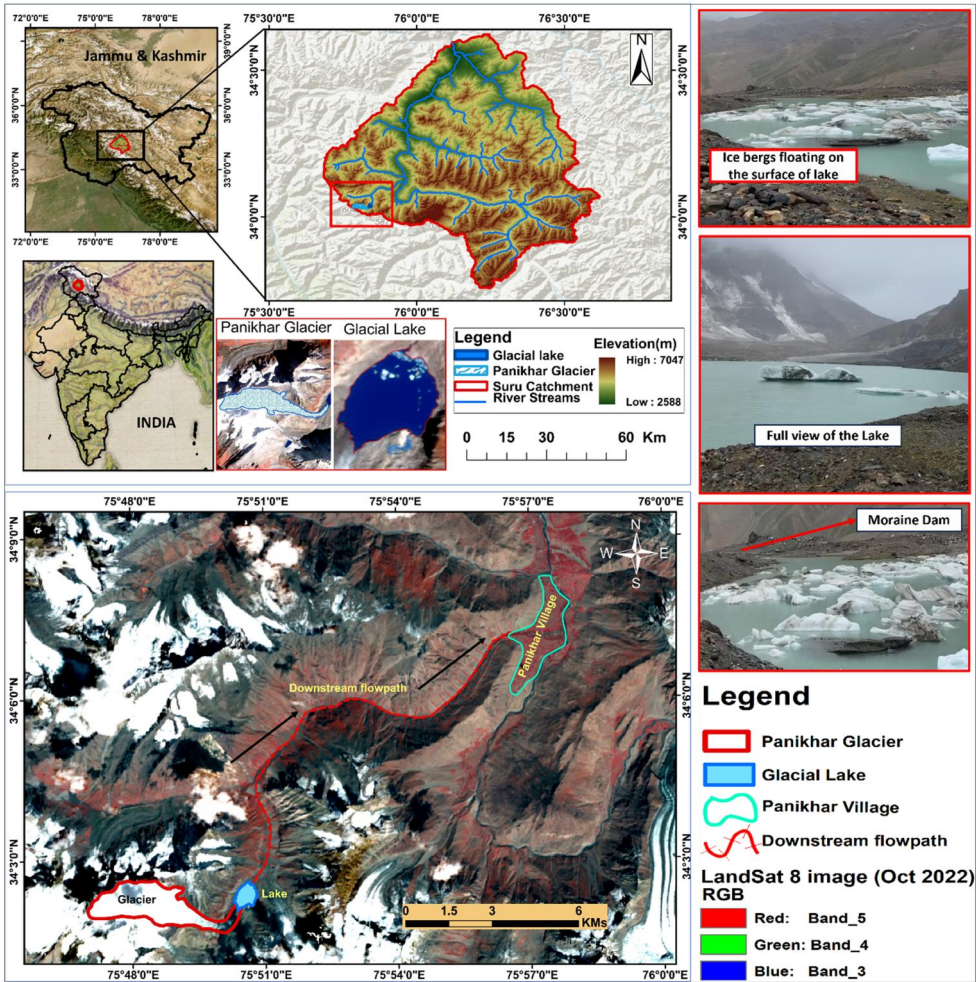


Figure 1. Location map of the Panikhar glacier, its proglacial lake and Panikhar village.

avalanches, which might catalyze a GLOF. The glacial lake is impounded by the glacier’s terminal moraine and the Panikhar settlement lies 13 km northeast of the glacial lake (Figure 2).

3. Datasets

This study used Sentinel-2A (10 m), PlanetScope (3 m), Landsat TM (30 m), Landsat ETM+ (30 m), and Landsat OLI (30 m) for the mapping of glacial lake and its mother glacier and estimating area changes in the glacial lake and its feeding glacier from 2000 to 2022. Moreover, high-resolution Google imagery was also used for verification and validation purposes. Advanced Land Observing Satellite (ALOS) Phased Array Synthetic-Aperture Radar (PALSAR) radiometrically terrain corrected (RTC) Digital Elevation Model (DEM) was downloaded online from <https://asf.alaska.edu> (accessed on 23rd May 2023), from which topographic information such as elevation, slope, aspect, hill shade, etc. was obtained. Furthermore, ASTER DEM (30 m) was

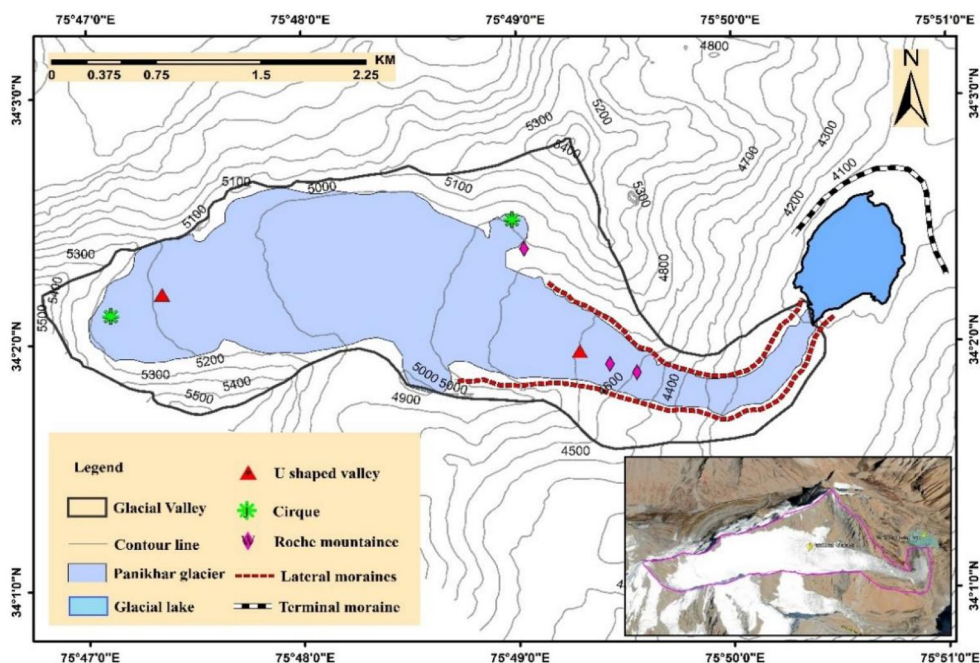


Figure 2. Glacial geomorphology of the study area.

Table 1. Datasets used in the study.

S. No	Data/Tool	Resolution	Year	Source
1.	Planet CubeSat	3m	2016, 2018, 2020, 2022	Planet https://www.planet.com/
2.	Landsat 7 ETM+	30 m	2000, 2010	USGS Earth Explorer http://www.earthexplorer.usgs.gov
3.	Landsat 8 OLI	30 m	2022	USGS Earth Explorer http://www.earthexplorer.usgs.gov
4.	Sentinel 2 A	10 m	2016, 2018, 2020, 2022	USGS Earth Explorer http://www.earthexplorer.usgs.gov/
5.	ALOS-PALSAR DEM	12.5 m	2015	https://asf.alaska.edu/
6.	SRTM DEM	90 m	2000	USGS Earth Explorer http://www.earthexplorer.usgs.gov/
7.	ASTER DEM	30 m	2022	https://www.earthdata.nasa.gov/
8.	Copernicus (GLO 30) DEM	30 m	2023	https://spacedata.copernicus.eu/collections
9.	Google Earth Imagery	<1 m	2000–2022	Google Earth Pro Tool
10.	CRU gridded data	0.5°	1990–2002	https://crudata.uea.ac.uk/cru/data/hrg

also used for glacier mass balance estimation through the geodetic method. PlanetScope imagery (3 m resolution) was acquired from the Planet Labs website www.planet.com. Landsat data was downloaded *via* the USGS Earth Explorer site, <https://earthexplorer.usgs.gov>, and Sentinel-2A images were obtained from the "Copernicus internet hub of European Space Agency" (ESA). Table 1 gives a summary of the datasets utilized in this study. These datasets have been extensively used in previous studies to analyze changes occurring on the Earth's surface (Ahmad et al. 2022a; Imdad et al. 2023; Malik et al. 2024; Mushtaq et al. 2024; Saleem et al. 2024).

4. Methods

4.1. Glacial lake mapping and change detection

We have employed Planet CubeSat RGB images to delineate the glacial lake outlines for the years 2016, 2018, 2020, and 2022. However, the Planet CubeSat data is available from the year 2016 onwards. Hence glacial lake outline delineation for 2000 and 2010 was carried out from Landsat 7 ETM+ images. Out of several techniques and approaches previously used for glacial lake mapping, we have employed an integrated approach using the normalized difference water index (NDWI) method coupled with manual digitization for the removal of any possible errors. NDWI is a widely employed method for the extraction of water pixels from a satellite image, using the difference in the reflectance values of Blue and Green bands (McFeeters 1996; Ahmed et al. 2022; Zhang et al. 2022; Rather et al. 2024a). However, the NDWI method faces certain issues while classifying pixels containing muddy patches, shadows, cloud cover, or ice (Kaplan and Avdan 2017; Wang et al. 2020; Ahmad et al. 2022b, Mir et al. 2022; Rather et al. 2024b). These issues were tackled through the generation of relief, slope, aspect, and hill shade maps from the ALOS Pulsar DEM accompanied by manual correction using high-resolution Google Earth imagery. Cloud cover acts as a major impediment in the process of mapping different features from satellite imagery, therefore, images were selected from the post-monsoon months. Wherever a cloud-free image was not available, images from the adjacent months were taken to address this problem. The high resolution of the Planet CubeSat images (3 m) proved helpful in the minimization of any errors in the lake boundary delineation.

4.1.1. Estimation of glacial lake depth, volume and peak discharge

A glacier lake's depth, volume, and peak flow are crucial factors in determining the GLOF threat connected to that specific glacial lake. For calculating the glacial lake depth and volume from satellite datasets, we have to rely upon certain empirical equations which are based on the glacial lake area, developed by researchers across the world. Field surveys of glacial lakes require enormous effort and resources owing to the harsh terrain of the Himalayan cryosphere; therefore, empirical equations are widely employed for this purpose (Evans 1986; Wang et al. 2011; Emmer and Vilímek 2013; Fujita et al. 2013). Several equations for the calculation of glacial lake depth, volume, and potential peak discharge have been developed which include those by Huggel et al. (2002), Wang et al. (2011), Qi et al. (2022), Patel et al. (2017), Fujita et al. (2013), etc. A summary of these equations is given in Table 2. To reduce bias, we computed the lake volume using these empirical equations and took the average of all the equations into account for the final result. For lake volume estimation the following equations: (Equations (1) and (2)), given by Qi et al. (2022), showed results closest to the average values. These equations use the geometry of the lake beside the lake area to calculate the lake volume.

For lakes larger than 0.1 km^2

$$V = 40.67^{1.184} - 3.218 \frac{mxw}{mxl} \quad (1)$$

Table 2. Empirical equations used for depth and volume calculations.

Empirical Equation	Parameter Calculated	Reference
$D = 0.104 \times A^{0.42}$	Lake Depth	Huggel et al. (2002)
$D_m = 55 \times A^{0.25}$	Lake Depth	Fujita et al. (2013)
$D_m = 4 \times 10^{-5} \times A + 5.0564$	Lake Depth	Patel et al. (2017)
$V = 0.104 \times A^{1.42}$	Lake Volume	Huggel et al. (2002)
$V = 0.035 \times A^{1.5}$	Lake Volume	Evans (1986)
$V = 0.0578 \times A^{1.4683}$	Lake Volume	(Liu et al., 2020)
$V = 40.67^{1.184} - 3.218 \frac{mxw}{mxl}$		
$V = 557.4^{2.455} + 0.2005 \frac{mxw}{mxl}$	Lake Volume	Qi et al. (2022)
$V = A \times D_m$	Lake Volume	Patel et al. (2017)
$Q_{max} = 0.00077 \times V^{1.017}$	Peak discharge	Huggel et al. (2002)
$Q_{max} = 0.72 \times V^{0.53}$	Peak discharge	Evans (1986)

For lakes smaller than 0.1 km^2

$$V = 557.4^{2.455} + 0.2005 \frac{mxw}{mxl} \quad (2)$$

4.2. Mapping the feeding glacier

We employed Planet CubeSat images along with Landsat 7 ETM+ and Sentinel 2 A imagery for mapping the feeding glacier of the lake. The Normalized difference Snow Index (NDSI) combined with visual interpretation was used for glacier area change detection analysis. NDSI method has been extensively used in the Himalayan cryosphere by several studies and is considered to be a reliable method for glacier mapping and change detection (Bolch et al. 2012; Kulkarni et al. 2012; (Paul et al. 2015)).

The error encountered in the estimation of glacier and lake areas is directly proportional to the resolution of the satellite images and it was evaluated using Equation (3).

$$A_{er} = 100 (n^{0.5} \times m) / A_{gl} \quad (3)$$

Where n is the ratio of the glacial lake's perimeter to the spatial resolution, m is the unit pixel area of the image (m^2), and A_{gl} is the glacial lake area (m^2).

4.2.1. Mass balance estimation of the glacier

Estimating the mass balance of glaciers can reveal important information about how glaciers behave in response to climate change and how glaciers interact with glacial lakes over a certain period. Various studies have employed different techniques to estimate the mass balance of glaciers globally (Soruco et al. (2009), Zemp et al. (2009), Barrand et al. (2010), Pratap et al. (2016) and Kumar et al. (2019) such as the glaciological method ((Kulkarni, 1992)), geodetic method (Kumar et al. 2017; Majeed et al. 2021), Hydrological method (Bhutiyan 1999; Pratap et al. 2016), etc. However, in this study, we conducted the mass balance estimation of the Panikhar glacier using the geodetic method as this is a convenient method to estimate mass balance keeping in view the harsh terrain of the region ((Rashid et al. 2020)). The basis of the geodetic approach is the calculation of the glacier's surface elevation difference over

time. This method computes the surface elevation difference or thickness change of the glacier using digital elevation models from different time periods. The glacier area and ice density assumptions are then used to translate the elevation change into mass loss. (Braithwaite 2002; Muhammad et al. 2019; Romshoo et al. 2023). SRTM DEM and ASTER DEM (30 m resolution), acquired from <https://www.earthdata.nasa.gov/> for the years 2000 and 2022 respectively, were used to calculate the elevation change of the glacier during this period using the DEM differencing technique. The DEMs were pre-processed in ArcMap 10.3 and the elevation difference was computed by comparing the elevation values of corresponding pixels from the two DEMs, using the raster calculator tool. The elevation difference was then translated into volume change using the cell size of the DEM. Assuming the ice density to be constant at 850 kg/m^3 , the mass loss from the glacier was calculated in kg/m^3 which was subsequently converted into meter water equivalent (m.w.e.).

4.2.2. Glacier surface velocity and ice thickness estimation

Surface velocities for the Panikhar Glacier were determined using the Glacier Image Velocimetry (GIV), a feature-tracking-based technique. GIV is a software package specifically designed for computing glacier velocity fields at high spatial resolution, utilizing unique points or characteristics on the glacier surface visible in consecutive satellite images. This meticulous process involves filtering individual velocity maps based on user-specified criteria, detecting and eliminating anomalous values using outlier detection functions, and computing statistical metrics for each grid cell over time. Sentinel-2 and Landsat true color composites were analyzed using GIV, with 20 multitemporal images with 30-meter spatial resolution from 2017 to 2023. Ice-thickness modeling during the same period utilized Copernicus DEM data at the same spatial resolution. Sentinel-2 images were used as input data for estimating glacier velocity, spanning from 2017 to 2023, with GIV configured to derive surface velocity considering a minimum temporal baseline gap of approximately 11 d and a maximum of three years. The displacement for each pair of images was computed using a multi-pass frequency domain cross-correlation algorithm, with subsequent filtering to remove pixels exceeding maximum velocity thresholds and enhancing result accuracy through spatial smoothing and rectification of systematic georeferencing errors using stable grounds.

The estimation of glacier thickness was conducted in MATLAB. For ice-thickness modeling, we employed the Copernicus DEM at the same spatial resolution. Our study adapted codes originally given by van Wyk de Vries et al. to suit our specific research requirements in our investigation of the Panikhar Glacier. We estimated ice thickness using an ice-velocity-based method. The equation follows the methodology proposed by (Gantayat et al., 2014), with further refinements by van Wyk de Vries et al. , particularly focusing on the mean slope and surface velocity computations.

$$H = \frac{4\sqrt{1 \cdot 5U_s}}{Af^3 (\rho g \sin \alpha)} \quad (4)$$

In this equation, H depicts the ice thickness, U_s denotes the surface velocity, f is the slope factor (often assumed as 0.8, especially suitable for Himalayan glaciers as noted by (Paterson, 1991)), g stands for the acceleration due to gravity (9.8 m/s^{-2}), α

signifies the glacier slope, and ρ indicates the ice density (typically taken as 900 kg/m^3 according to (Farinotti et al., 2009)).

Glacier volume estimation adopted a piece-wise method, involving the summation of the product of the squared ground pixel size and its respective ice thickness. In Equation (5), $H_{j,k}$ represents the mean value of each pixel in the ice-thickness map, while r depicts the ground resolution of the pixel, assuming square pixels applicable to optical remote sensing data.

$$V_p = \sum_{j=1}^{n_j} \sum_{k=1}^{n_k} H_{j,k} \times r^2 \quad (5)$$

4.3. GLOF hazard analysis

In the Himalayan region, a widely used method for determining GLOF vulnerability is predictive analysis utilizing a multicriteria framework (Bolch et al. 2008; Wang et al. 2011; Worni et al. 2013; Rounce et al. 2017; Wang et al. 2018; Dubey and Goyal 2020; Khadka et al. 2021; Ahmed et al. 2022). Despite the extensive use of this method in GLOF investigations, this method involves some amount of subjective expert judgment. This is because the GLOF susceptibility analysis is a complex process, and local variations in the influencing criteria make it nearly difficult to develop a uniform framework for this purpose globally (Allen et al. 2019; Taylor et al. 2023). In this study, we adopted the framework given by Che et al. (2014) as found to be suitable in our study area. This framework includes 10 relevant criteria pertaining to the glacial lake and its surrounding conditions that affect GLOF susceptibility and classifies the lakes into 5 levels of hazard from level 1 to level 5 using the weighted sum method (Table 3).

4.4. GLOF modeling

The two-dimensional (2D) GLOF modeling of the lake was done using HEC-RAS 2D (Version 6.3.1) to simulate two distinct scenarios: piping and overtopping. The aim was to assess the potential flood impacts from the glacial lake on the nearby downstream settlements. This approach has been extensively used to model the GLOF events globally as well as in the Himalayan region (Klimeš et al. 2014; Worni et al.

Table 3. Integrated criteria used for assessing GLOF hazard, adopted from Che et al. (2014).

Index	Criteria	Weight	Criteria Presence
Type of glacial lake	Terminal moraine dammed lake	0.15	Yes
Area of lake	$>0.2 \text{ km}^2$	0.15	Yes
Distance between lake and its mother glacier	$<500 \text{ m}$	0.15	Yes
Average slope of the glacier	$>7^\circ$	0.10	Yes
Slope of the downstream	$>20^\circ$	0.10	No
Top width of the dam	$<60 \text{ m}$	0.10	No
Area of the glacier	$>2 \text{ km}^2$	0.09	Yes
Slope between lake and its mother glacier	$>8^\circ$	0.07	No
Change of lake area	$>10\%$ in a decade	0.06	Yes
Elevation of the lake	$>5000 \text{ m}$	0.03	No

2014; Sattar et al. 2019; Sattar et al. 2021; Majeed et al. 2021; Ahmed et al. 2022; Rawat et al. 2023b).

4.4.1. Model input and setup

HEC-RAS requires a digital elevation model (DEM), for providing detailed terrain data for the study area. This raster-based DEM serves as the foundation for defining the flow area of interest, spanning from the glacial lake to the vulnerable settlements downstream. Within this defined flow area, a 2D computational mesh is constructed using cells of uniform dimensions. Each cell in the mesh is characterized by: Manning's roughness coefficient (N value), representing the flow resistance and the elevation data extracted from the DEM, specifying the terrain height at each cell location. ALOS PALSAR DEM was employed in this study given its better spatial resolution of 12.5 meters.

4.4.2. Simulating two different GLOF failures

- a. **Piping Failure:** This scenario simulates the failure of the lake dam or natural barrier due to internal erosion (piping). The modeling process involves steps like defining an initial breach hydrograph corresponding to the piping failure, setting the boundary conditions to initiate breach formation, and simulating flood propagation downstream. The 2D hydrodynamic modeling approach captures the breach evolution and flood wave propagation characteristics along the flow path. The characteristics of the potential flood wave were simulated for two different case scenarios presuming 50% and 100% drainage of the lake respectively.
- b. **Overtopping Failure:** In overtopping failure, flood generation occurs when water levels exceed the capacity of the dam or barrier, causing water to spill over the top. The modeling procedure includes defining an appropriate initial breach hydrograph corresponding to the overtopping event and configuring the boundary conditions to simulate breach initiation and the subsequent flood wave propagation downstream. This is followed by employing the 2D hydraulic model to capture the breach dynamics and the flood wave behavior, considering terrain elevations and flow resistances. This was also done keeping in view the moderate and worst-case scenarios with 50% and 100% volume of the lake.

4.4.3. Model outputs and analysis

The 2D modeling process generates spatially distributed outputs including water depth distribution, flow velocity profiles indicating flood wave dynamics, and inundation extents depicting areas affected by the flood waters. These outputs enable detailed analysis of flood impacts along the route from the Lake to the settlements for both piping and overtopping scenarios. By integrating terrain data, hydraulic properties, and the breach conditions, the modeling study provides critical insights into potential flood hazards and helps in the development of mitigation frameworks for disaster preparedness and response. This comprehensive approach leverages advanced hydraulic modeling techniques to simulate complex flood scenarios, facilitating informed decision-making and risk assessment in vulnerable regions prone to GLOF events.

5. Results

5.1. Depth, volume, and peak discharge of the lake

The glacial lake depth and volume estimations were carried out using the various regression equations stated in Table 4. The results of these equations vary considerably and hence an average value of all of these equations was considered as the final estimate of lake depth and lake volume to minimize the bias in the final estimates as suggested by Emmer (2018). Using this approach, the average depth of the lake was estimated as 31.50 m while the average volume was estimated as $14.04 \times 10^6 \text{ m}^3$. The equation developed by Fujita showed exaggerated estimates of lake depth in comparison to the other equations and in calculating the lake volume, the maximum value was obtained through Liu's equation while Qi's equation showed results closest to the average value of all equations.

The estimation of the Peak discharge of the lake was done using the equations given by Huggel et al. (2002) and Evans (1986), and the values obtained from these equations are recorded in Table 4. To minimize the bias, the average value of these two equations, which came out to be $7954.19 \text{ m}^3 \text{ s}^{-1}$, was taken as the final estimate of the peak discharge of the lake as suggested by Emmer et al. (2018).

5.2. Glacial lake area change

The change detection analysis of the lake, using multi-temporal datasets, revealed an overall increase of 78.72% in the lake's area at a rate of 0.017 km^2 per annum. The lake area has gone up from $0.10 \text{ km}^2 \pm 75.9 \text{ m}^2$ in 2000 to $0.22 \text{ km}^2 \pm 0.82 \text{ m}^2$ in 2010, $0.33 \text{ km}^2 \pm 0.82 \text{ m}^2$ in 2016, $0.37 \text{ km}^2 \pm 0.72 \text{ m}^2$ in 2018, $0.41 \text{ km}^2 \pm 0.67 \text{ m}^2$ in 2020 and $0.47 \text{ km}^2 \pm 0.62 \text{ m}^2$ in 2022. The lake area has witnessed an overall increase of $\sim 0.37 \text{ km}^2$ in the past 22 years. It has almost doubled in each decade from 2000 to 2020 which depicts a very rapid expansion scenario, much likely to accelerate further in the future decade of 2020–2030 keeping in view the increasing temperature trends in the region. Figure 3 depicts the expansion of the lake through lake outline maps.

5.3. Changes in the feeding glacier of the lake

5.3.1. Area changes

The feeding glacier of Panikhar Lake was also subjected to spatio-temporal change detection analysis. The results revealed a significant decrease of $\sim 0.61 \text{ km}^2$ in the glacier area accounting for a 13.2% overall decrease in the glacier area for the past

Table 4. A summary of various equations used for depth and volume measurements.

Emp. Equation	Depth (m)	Volume (10^6 m^3)	Peak Discharge (m^3/s)
Huggel	25.08	11.78	11,963.14
Fujita	45.58	–	–
Evans	–	11.33	3945.24
Liu	–	19.17	–
Qi	–	14.43	–
Patel	23.86	11.21	–
Average Value	31.50	14.04	7954.19

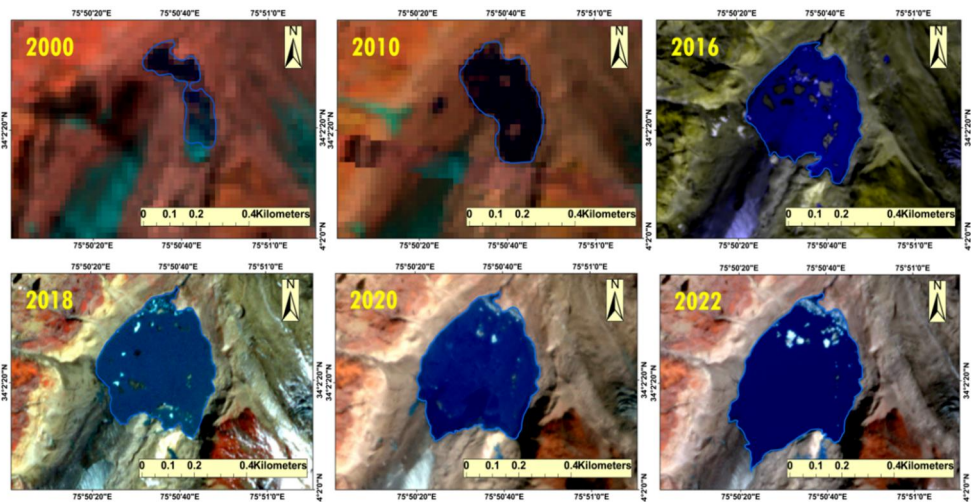


Figure 3. Expansion of Panikhar glacial lake from 2000 to 2022 depicted on Planet CubeSat (RGB) and Landsat 7 ETM+ images.

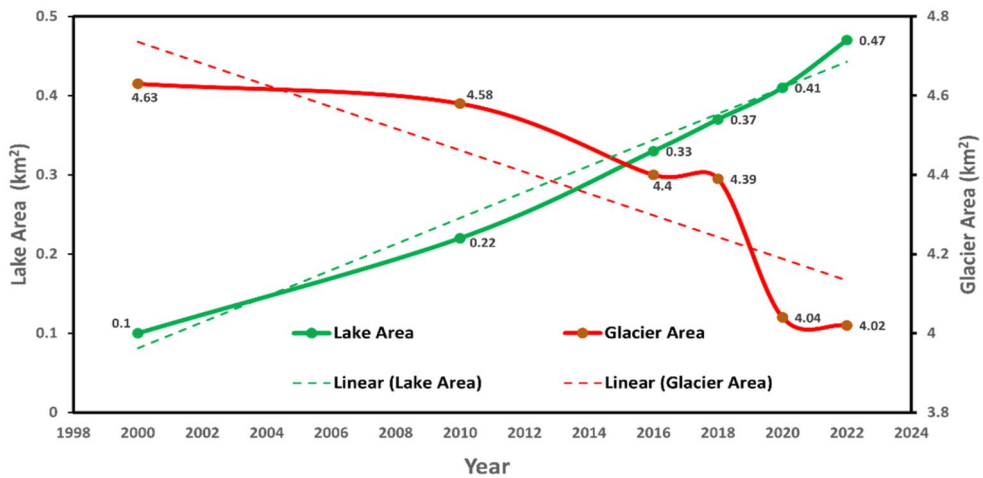


Figure 4. Glacier and glacial lake area trends.

22 years. The overall area of the glacier has decreased from $4.63 \text{ km}^2 \pm 139 \text{ m}^2$ in 2000 to $4.58 \text{ km}^2 \pm 138.4 \text{ m}^2$ in 2010, $4.50 \text{ km}^2 \pm 0.01 \text{ m}^2$ in 2016, $4.39 \text{ km}^2 \pm 0.01 \text{ m}^2$ in 2018, $4.04 \text{ km}^2 \pm 0.02 \text{ m}^2$ in 2020 and $4.02 \text{ km}^2 \pm 0.02 \text{ m}^2$ in 2022 with an annual decrease rate of $\sim 0.03 \text{ km}^2$ (Figures 4 and 5). The glacier has witnessed a snout retreat of 348 m in this period. The glacier and the glacial lake areas behold a reciprocal relationship with each other which means that the glacial lake is expanding at the expense of its feeding glacier (Figure 4).

5.3.2. Mass balance of the glacier

The glacier mass balance was estimated through the geodetic method and the results reveal that the glacier has, on average, undergone a thickness loss of 7.04 m from 2000

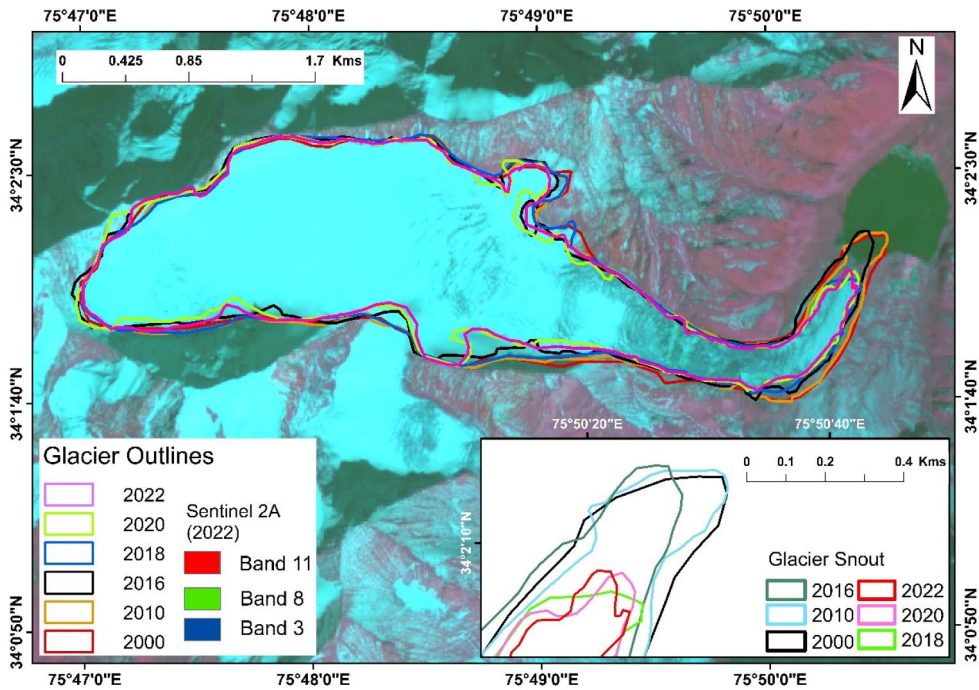


Figure 5. Spatio-temporal evolution of the Panikhar glacier for the last 22 years.

to 2022 at the rate of 0.32 m a^{-1} . The total mass balance of the glacier was estimated to be -5.922 m w.e. which amounts to a total mass loss of ~ 5.92 metric tons per square metre during this period at the rate of 0.27 metric tons per square metre per year (Figure 6). The mass balance values across the glacier fall from -0.05 m w.e. to 0.06 m w.e. with a mean negative value. This depicts that despite certain accumulation regions on the glacier, the glacier has an overall negative mean mass balance. These results are in proximity to other studies in the region. For instance, Kumar et al. (2017) reported an annual mass balance of $-0.53 \pm 0.16 \text{ m w.e.}$ per year for the glaciers in the Western Himalayas. Majeed et al. (2021) reported a mass balance of -0.24 m w.e. per year for clean glaciers and -0.37 m w.e. per year for debris-covered ones in the Pangong region.

5.3.3. Surface velocity, ice thickness, and volume of the glacier

According to the velocity estimations, the glacier's mean velocity was estimated to be 3.38 m a^{-1} , while its surface velocity varied from 0.87 m/y to 9.76 m a^{-1} . (Figure 7a). The glacier is characterized by a slowly moving snout with slightly increasing velocities in the upper accumulation zone. Previous studies in the region also report the existence of an increasing trend in the surface velocity of the glaciers with increasing elevation until a maximum is reached towards the transient snow lines (Bhushan et al. 2018; Ahmed et al. 2022).

The ice thickness measurement of the glacier, conducted in MATLAB, reveals that the thickness of the glacier varies from 14.39 m to 50.87 m (Figure 7b) while the mean thickness was estimated to be 30.95 m . The thickness of the glacier increases

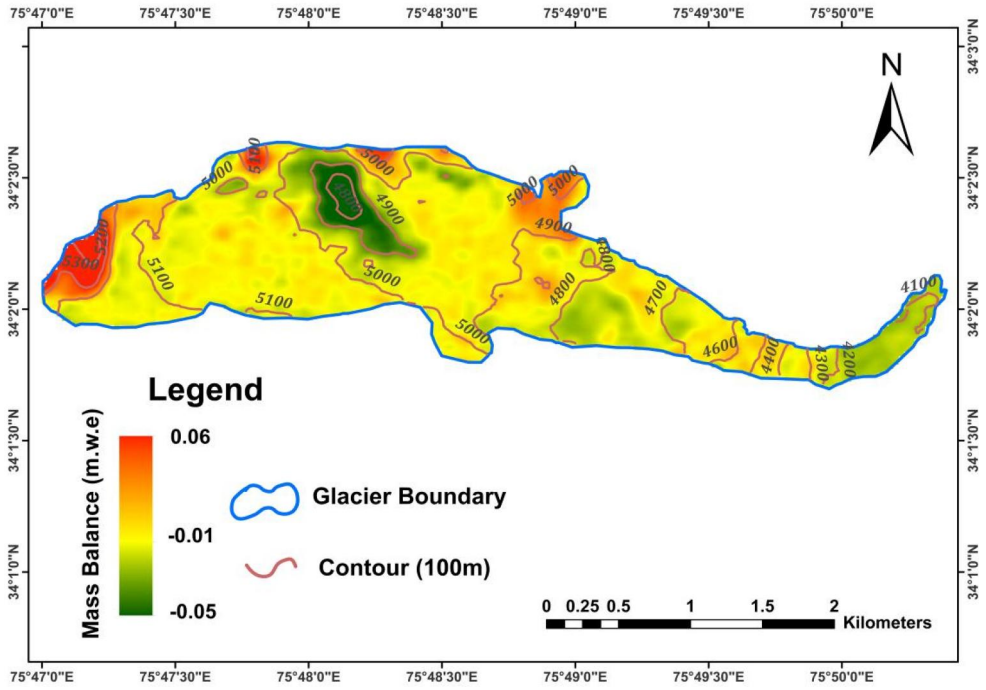


Figure 6. Spatial variation of geodetic mass balance across Panikhar glacier in meter water equivalent (m.w.e).

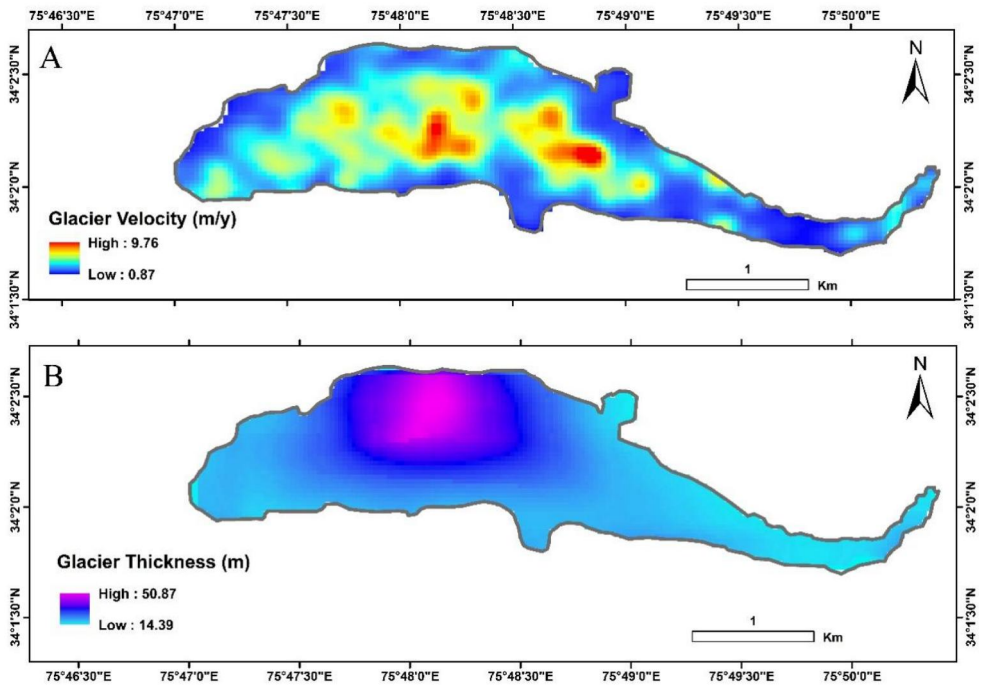


Figure 7. Figure depicting (A) glacier surface velocity and (B) ice thickness distribution.

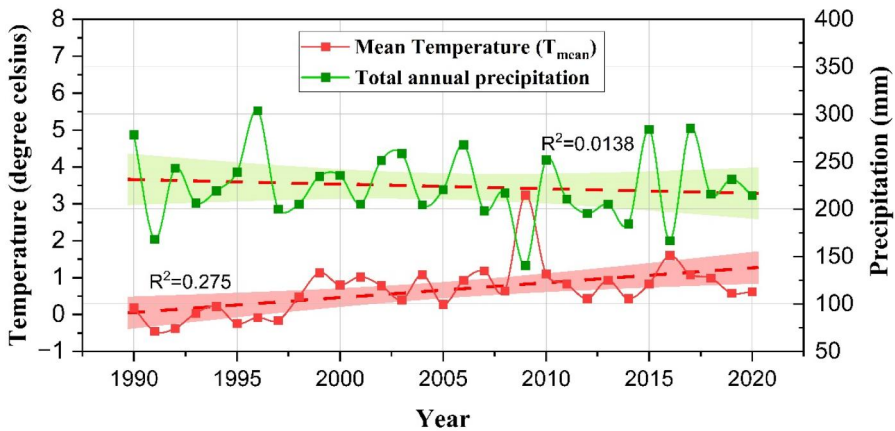


Figure 8. Temperature and precipitation trends in Ladakh.

towards the center and decreases as we move towards the edges. The total glacier volume as estimated from the thickness estimates and the glacier pixel areas was found to be $45,783 \text{ m}^3$.

5.4. Temperature and precipitation variability over the region

The Ladakh region is overall a data-scarce region with only a few observatories for the generation of observed temperature and precipitation data. Keeping this in mind, we projected the trends in the mean annual temperature (T_{mean}) and Total annual precipitation in the region using a gridded climatic dataset given by the Climate Research Unit (CRU) to peek into the climatic controls of the glacial lake expansion. It was found that the mean annual temperature has witnessed a slight positive trend ($R^2 = 0.275$) during this period while the total annual precipitation in the region has witnessed a slight negative trend with an R^2 value of 0.0138 (Figure 8).

The warming temperature trends in this region and declining precipitation trends are also confirmed by previous studies that use various gridded climate data products to analyze the climatic variability in Ladakh (Shafiq et al. 2016; Ahmad et al. 2019; Mann et al. 2022). This may lead to further glacier recession and subsequent glacial lake expansion in the near future making the local populations vulnerable to cryospheric disasters such as the GLOF.

6. GLOF risk

6.1. GLOF susceptibility analysis

We carried out the GLOF susceptibility analysis of the glacial lake based on the approach used by Che et al. (2014) which includes criteria pertaining to both the lake and the surrounding conditions that affect GLOF susceptibility (Table 3) and classifies the lakes into 5 levels of hazard from level 1 to level 5. The lake was found to be a High-hazard lake associated with a level 4 hazard. Some of the major reasons that account for the high hazard index of the lake are its large size, unstable moraine dam, direct connection to its mother glacier, marked rate of expansion, and a large-

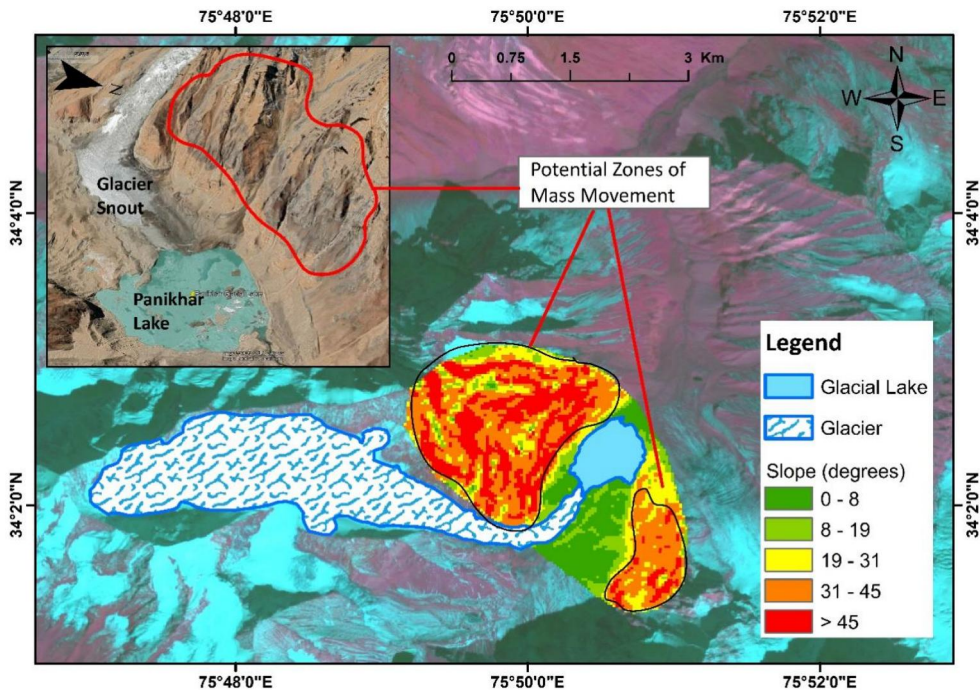


Figure 9. The local topographic setting of the Panikhar glacier-lake complex and zones of possible mass movement.

sized mother glacier (4.02 km^2) with a slope of 16.5° . Moreover, the lake is prone to rock fall/debris fall from its adjoining steep slopes as evident from the slope profile of the lake surroundings (Figure 9).

6.2. Hydrodynamic modelling

We analyzed the potential impacts of an outburst event originating from the Panikhar Lake by analyzing the temporal and spatial properties of the flood wave using two-dimensional hydraulic modeling for two different case scenarios. In scenario 1, we assumed that 50% of the total volume of the lake is drained whereas scenario 2 was the worst-case scenario assuming a 100% drainage of the lake.

6.2.1. Scenario 1: assuming 50% water volume of the lake is released

Given the dynamic nature of high-magnitude flood events, we focused on understanding the changing hydraulic properties over time, particularly examining discharge, flow velocity, and depths across the flow channel. Assuming drainage of 50% of the lake's total water volume, we found that the maximum discharge at the point of the breach was $1908.25 \text{ m}^3/\text{s}$ and $3271.50 \text{ m}^3/\text{s}$ for the piping and overtopping failures respectively (Figure 10a). The routed hydrographs depict that the flood wave in this scenario will reach the first settlement in 1 h and 4 min after the dam breach in both the piping and the overtopping failures with a peak discharge of $2701.1 \text{ m}^3/\text{s}$ and $2714.7 \text{ m}^3/\text{s}$ respectively (Figure 11a). The flood depths along the flow path are

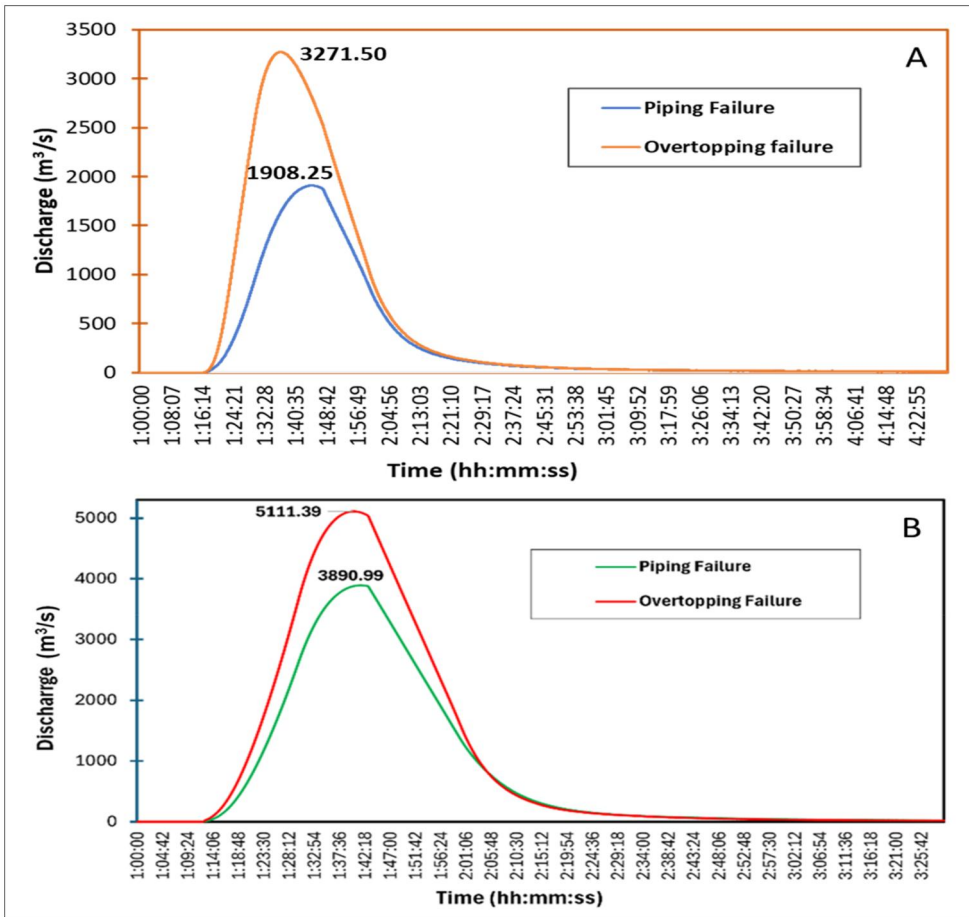


Figure 10. Breach hydrographs depicting peak discharge at the breach in piping and overtopping failures (A) 50% volume of the lake (B) 100% volume of the lake (worst case scenario).

depicted in Figure 12. The maximum flood velocity was estimated to be 18.26 m/s while the maximum depth of the flood wave was found to be 14.87 m.

The maximum area under the threat of inundation along the valley was calculated as 4.74 km² for both the overtopping and piping failure situations. The mean flood depth across the flow channel was estimated to be 3.41 meters and the mean flood velocity was found to be 3.84 m/s. We found that the potential flood wave in this scenario inundates bridges, roads, and a few residential houses along the channel in settlement 2 and near the Suru Valley bridge (Figure 13).

6.2.2. Scenario 2: assuming 100% water volume of the lake is released

The maximum discharge, in the worst-case scenario with 100% water release, at the point of breach was calculated to be 3890.99 m³/s and 5111.39 m³/s for the piping and overtopping scenarios respectively (Figure 10b). A routed flood wave in the simulation reached the closest settlement (settlement 1) of the Panikhar village in 50 min after the lake-breach event with a peak discharge of 6345.06 m³/s and 6453.9 m³/s for the piping and overtopping scenarios respectively (Figure 11b).

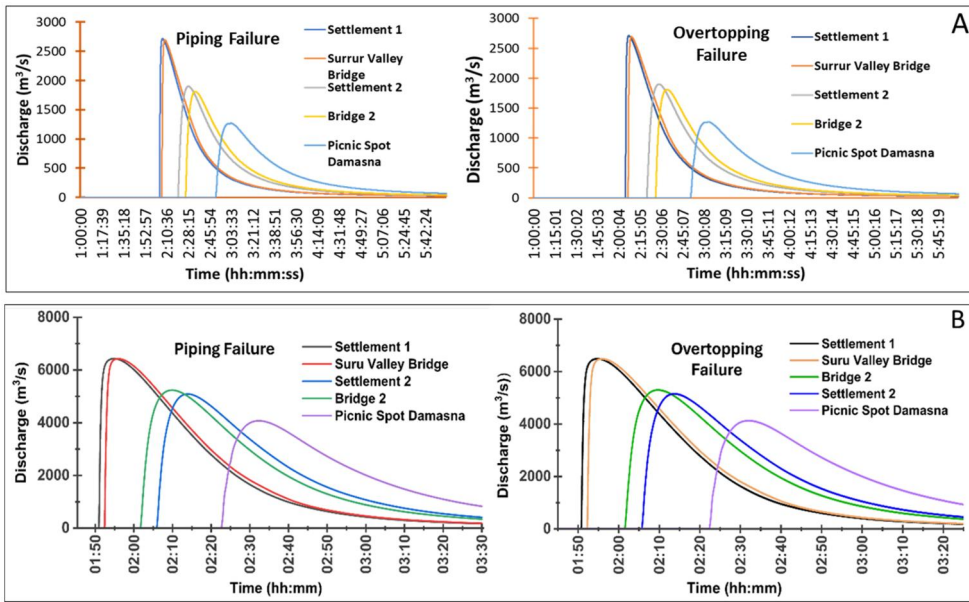


Figure 11. Routed hydrographs at various locations along the downstream flow channel in piping and overtopping failures (A) Assuming release of 50% of the water volume of the lake (B) Assuming release of 100% of the water volume of the lake.

The two-dimensional routing of the breach hydrograph is simulated over a distance of 25.6 km along the flow channel, from the lake to the Damasna picnic spot in Panikhar village. The maximum area under the threat of inundation along the valley was calculated as 5.38 km² for both the overtopping and piping failures (Figure 16). Across the entire channel, the mean flow discharge and mean flow depth are recorded at 588 m³/s and 5.31 m for piping failure 755 m³/s, and 5.33 m for overtopping failure with a mean flow velocity of 5.37 m/s. The flood depth and velocity vary along the flow channel as per the terrain profile of the flow channel (Figure 13). The flood depth and velocity values decline towards the lower reaches of the flow channel, as a result of the increase in the channel width and decrease in the slope.

The potential flood wave inundates infrastructure such as roads, bridges, and settlements along the channel with varying depths and velocities for both the piping and overtopping failures (Figures 14 and 15, Table 5). We evaluated the flood depths and flood velocities along the flow channel at settlements 1 and 2 to determine the maximum flood depths, peak flood velocities, and the time of the peak. Settlements 1 and 2 witness the highest potential flood depths of 7.9 and 7.65 m in the overtopping scenario whereas the lowest flood depths are witnessed at the Damasna picnic spot. Settlement 1 witnesses the highest peak velocities of 12.36 m/s and 11.35 m/s in the Piping and the overtopping scenarios (Figure 15).

7. Discussion

The Himalayan region is a hotspot of GLOF risk (Taylor et al. 2023) and this risk is projected to increase three times by the year 2100 (Zhang et al. 2024). 18% of all the

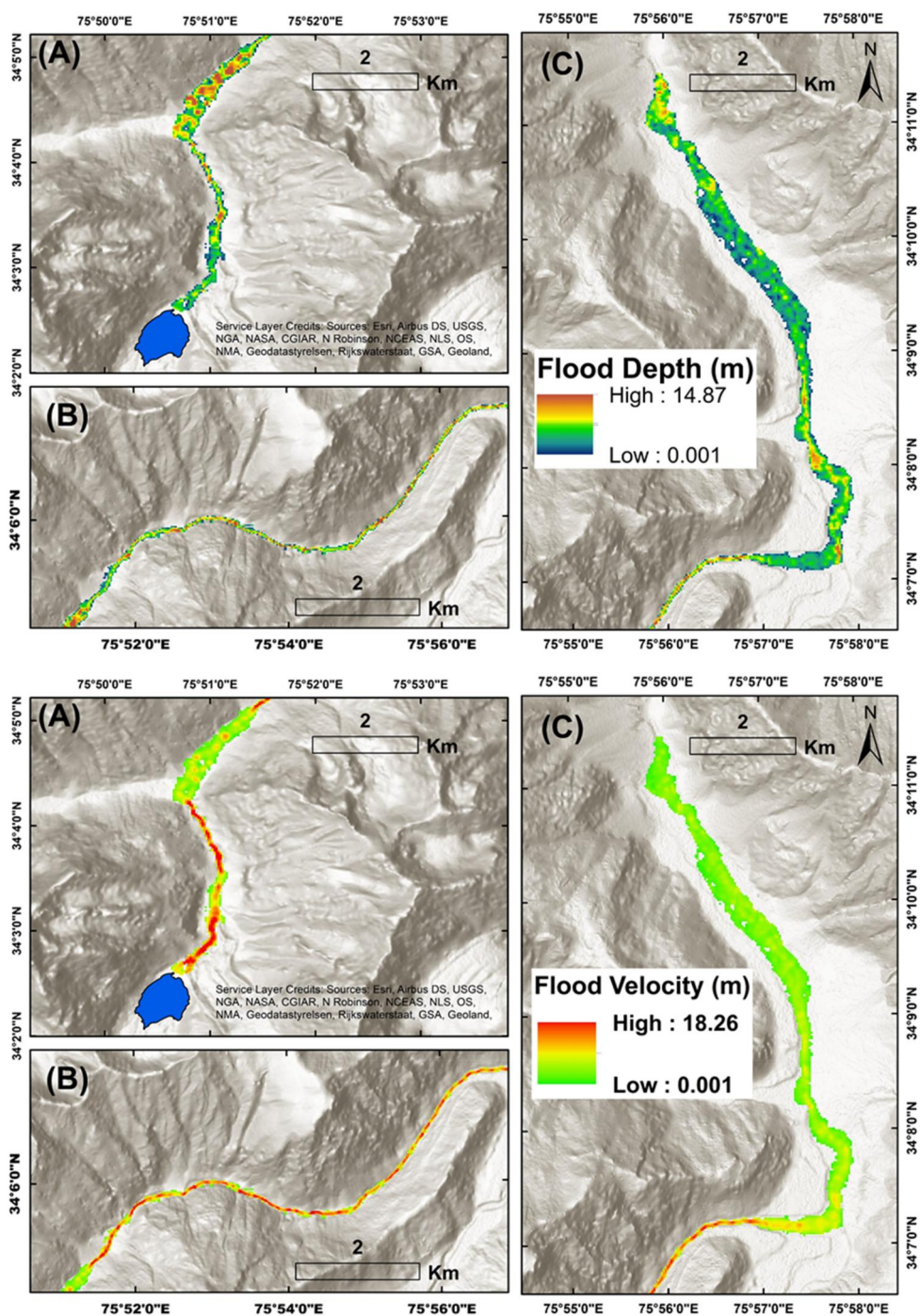


Figure 12. Flood depth and velocity profiles in the downstream flow channel in the first case scenario (50% volume). Parts A, B and C represent the 1st, 2nd and 3rd sections along the flow channel.



Figure 13. Buildings, roads, bridges and other infrastructure under potential threat of GLOF inundation in scenario (1) in the downstream flow channel of Panikhar lake.

previous GLOF events have occurred in the High Mountain Asia (HMA) which includes the Himalayan region. Most of the GLOF events in Himalayan region have been reported from the moraine and ice-dammed glacial lakes (Shrestha et al. 2010). The key triggers of GLOF in the region are extreme precipitation events and mass movements such as ice avalanches (Shrestha et al. 2010; Zhang et al. 2024). The rapid expansion of mountainous populations into high-risk zones is one of the major contributors to increasing GLOF risk in this region (Taylor et al. 2023). A large body of literature has been produced by researchers to generate baseline data about the GLOF phenomenon in the data-scarce Himalayan region (Emmer et al. 2022). These studies have focused on the preparation of glacial lake inventories, identification of potentially dangerous glacial lakes, and estimation of GLOF risk associated with hazardous lakes.

Categorizing a lake as potentially dangerous is very difficult given the multitude of factors influencing a GLOF event such as lake size, lake dam, lake surroundings, landslide, avalanche susceptibility, or extreme weather event. Therefore, under particular circumstances, an otherwise stable lake can also produce a GLOF event. Extreme precipitation events have caused notable GLOF events in the past through dam overtopping or collapse. This adds to the complexity of understanding and predicting the GLOF disaster. The same problem arises with the categorization of glacial lakes as potentially dangerous or otherwise based on size. Generally, some area threshold (e.g. $A > 0.1 \text{ km}^2$) is defined to exclude smaller lakes from the list of potentially dangerous lakes. For instance, Worni et al. (2013) did not classify the Gya Lake in Ladakh as potentially hazardous, maybe because it was ice-covered or because its size was below the mapping threshold of the study (0.01 km^2), leading to the assumption that it did not pose any significant threat to the settlements downstream. It can be challenging to leave out lakes that may be dangerous, as the same was demonstrated by the 2013 Chorabari lake outburst event (Das et al. 2015; Bhambri et al.

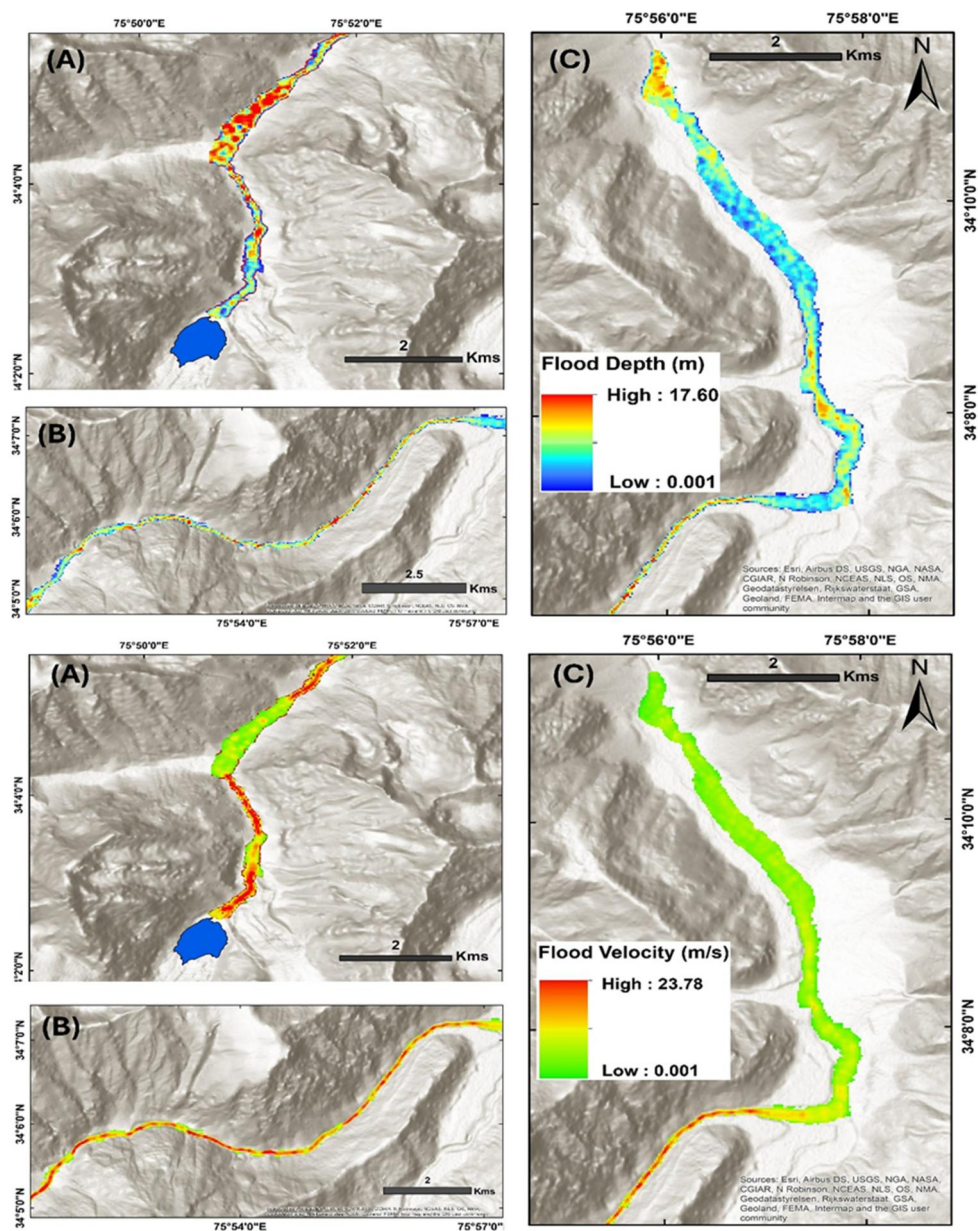


Figure 14. Flood depth and velocity profiles in the downstream flow channel in the worst case scenario (100% volume). Parts A, B and C represent 1st, 2nd and 3rd sections along the flow channel.

2016). According to several studies, small glacial lakes have the potential to seriously harm local livelihoods and cause major problems, as demonstrated by the Domkhar food in Ladakh (Ikeda et al. 2016) and other minor foods in Hunza region (Ashraf et al. 2021). The triggering factors of the GLOF are often dynamic and may change from time to time both quantitatively and qualitatively and hence require regular monitoring. e.g. Lakes that are stable as such, may get exposed to unstable

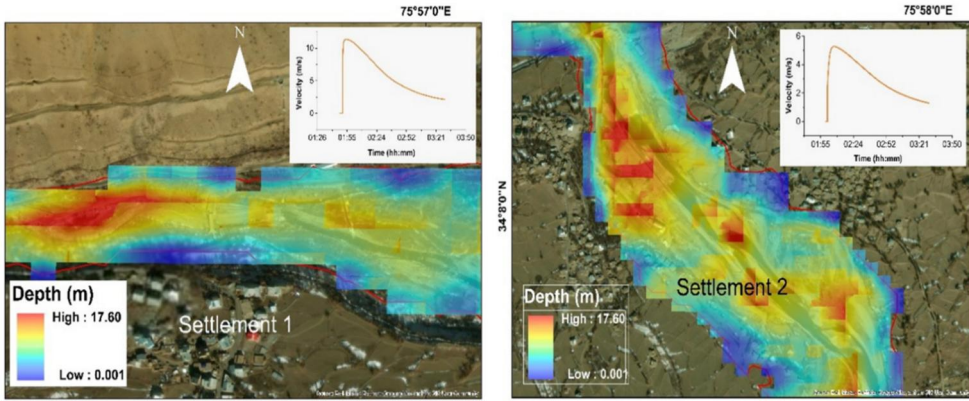


Figure 15. Flood depth and flood velocity curves at settlements 1 and 2 in Panikhar village.

Table 5. Flood parameters at various locations of the flow path downstream of Panikhar lake for the worst case scenario i.e.100% water release.

Location	Distance from the Lake (km)	Mean Depth (m)	Overtopping Failure		Pipping Failure		
			Max Depth (m)	Peak Velocity (m/s)	Mean Depth (m)	Max Depth (m)	Peak Velocity (m/s)
Settlement 1	15.6	4.35	7.97	11.35	3.05	6.61	12.36
Suru valley Bridge	16.11	2.25	4.16	9.05	1.96	4.29	8.66
Settlement 2	18.01	4.63	7.65	5.27	4.71	7.67	3.70
Bridge 2	19.08	2.73	5.33	5.82	1.97	3.99	5.36
Picnic Spot Damasna	22.50	1.70	6.96	6.615	5.13	6.70	7.187

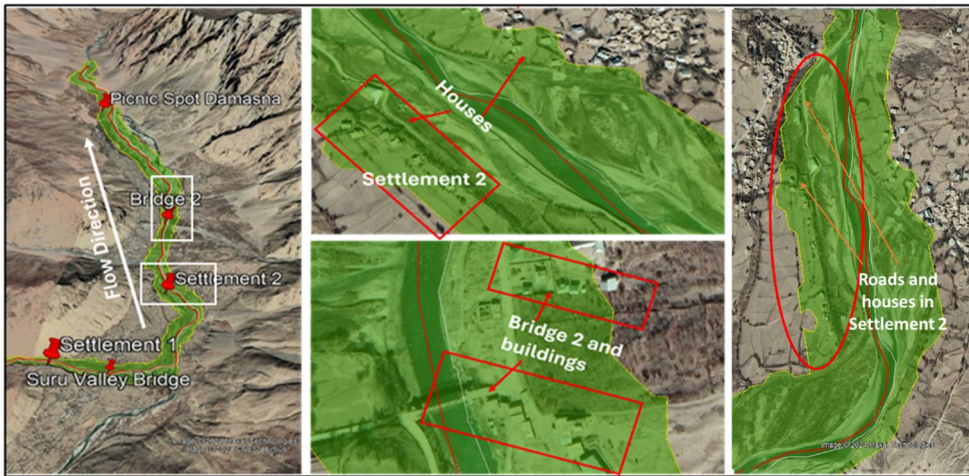


Figure 16. Inundation area in scenario 2 (100% water release) with some important areas with buildings, roads, bridges and other infrastructure under potential threat of GLOF inundation.

surrounding slopes or ice avalanche zones after expanding into the glacial valleys thus enhancing their susceptibility (Haeberli et al., 2017).

As moraine and ice-dammed lakes are more vulnerable to GLOF, they should receive greater attention when it comes to GLOF prioritization. Also, lakes that are in close proximity to the parent glacier are more likely to produce a GLOF as these lakes are more at threat of Icefalls and glacial calving activity. The likelihood of piping activity leading to a dam collapse is higher in lakes with underground drainage (Narama et al. 2018). Additionally, because thermokarst processes may block the intra-moraine channels, which can result in overflow and subsequent lake outburst through breaching, glacial lakes with subterranean drainage are more prone to GLOFs unlike the ones with stable surface drainage (Narama et al. 2018; Petrakov et al. 2020). Lakes with smaller dam width-to-height ratios and lower freeboard levels should be the focus of the GLOF study as they are important indicators of the dam's stability and can be estimated using high-resolution satellite imagery.

Studies similar to the present study had been previously conducted for the South-Lhonak Lake in Sikkim, which, later on, witnessed a severe GLOF event this year killing at least 40 people. However, effective measures were not taken to prevent this disaster which could have been easily done through certain practical measures taken on time. To avoid such tragedies in the future, a closer examination of the GLOF hazard is necessary, aided by more precise tools and dependable datasets. However, scientific knowledge of the environmental processes at play in the Himalayan region is often hampered by the sparse network of monitoring sites required to generate an ample amount of reliable meteorological and glaciological data. Regularly updated weather data coupled with high-resolution imagery, DEMs and detailed inventories can help in understanding the processes of the Himalayan cryosphere much more closely to prevent any future disasters. In addition to fine satellite datasets, bathymetric surveys are needed to estimate lake volumes more precisely because, even in similar geographic locations, lakes' sizes are not always equally predictable (Cook and Quincey 2015). Although there are numerous empirical equations devised for the estimation of the depth and volume of the lakes, there is always a chance of over or underestimation of these attributes. Hence bathymetric datasets can be extremely helpful in the estimation of the lake volume and the potential maximum discharge from a glacial lake in case of a GLOF event.

Mapping the societal elements of risk associated with the GLOF disaster is a largely ignored domain in the Himalayan region. At the national and state levels, GLOF risk profiles, that map the exposure and vulnerability of human life and property to this specific cryospheric danger must be produced and regularly updated. India lacks an early warning system infrastructure for the GLOF disaster even when the northern and the northeastern states of the country are under serious GLOF danger. Hence effective early warning systems need to be installed at critically hazardous glacial lakes that will help in evacuating the vulnerable population at the time of a future GLOF disaster and evading major risks associated with human life and key infrastructure such as the hydroelectric projects.

8. Conclusion

The glacier-lake interactions were studied for the Panikhar glacial lake and its feeding glacier for the past 22 years. We found that the glacial lake has undergone a remarkable expansion during this period. The area of the lake has increased by 0.37 km^2 , from

~0.10 km² in 2000 to ~0.47 km² in 2022, showing a net increase of 78.7%, at the rate of 0.017 km² per year while as its mother glacier has retreated significantly from ~4.63 km² in 2000 to ~4.02 km² in 2022 showing a total decrease of 13.2% in its total area i.e. 0.03 km² per annum. The glacier and glacial lake area plots show an inverse relationship which shows that the glacial lake is rapidly expanding at the expense of its mother glacier. The mass balance estimate of the Panikhar glacier also reveals a mass loss of 5.92 metric tons per square metre and an average thickness loss of 7.04 m over the past 22 years. The glacial lake is impounded by the terminal moraine of the glacier, rendering it hazardous, due to its swift rate of expansion and various other contextual factors. Notably, the presence of zones susceptible to potential mass movement in the surrounding areas also contributes to the heightened risk associated with this lake. The mean surface velocity and thickness of the glacier were estimated to be 3.38 m s⁻¹ and 30.95 m respectively. The potential outburst flood was modeled for two different GLOF scenarios using the HEC-RAS tool to generate flood depth and velocity profiles along the flow path for a distance of 25 km. The results reveal that the glacial lake is a potential threat to the downstream villages, especially the nearby Panikhar village. A total area of 5.38 km² which includes key infrastructure such as settlements, bridges, and roads is vulnerable to a potential GLOF event in the worst-case scenario. The routed hydrographs indicate that the flood wave generated at the time of an overtopping failure will arrive at the nearest settlement in 50 min with a peak velocity of 12.36 m/s. This study suggests regular monitoring of the lake and the installation of an early warning system (EWS) to mitigate and manage the risk from the lake in the future, especially at the time of an extreme weather event.

Acknowledgments

The first author gratefully acknowledges the financial support provided by the University Grants Commission (UGC) through the Senior Research Fellowship (SRF). This support was instrumental in the successful completion of this research.

Ethical approval

All the ethical standards of research publishing were taken care of during this study.

Disclosure statement

No potential conflict of interest was reported by the author(s).

Funding

No funding was received to conduct this study.

References

Ahmad L, Parvaze S, Sheraz Mahdi S, Kanth RH. 2019. Climate scenario in cold arid region and its future prediction. In: Mahdi SS, editor. Climate change and agriculture in India: impact and adaptation. Srinagar: Springer; p. 239–250.

- Ahmad ST, Ahmed R, Wani GF, Sharma P, Ahmed P, Mir RA, Alam JB. 2022a. Assessing the status of glaciers in upper Jhelum Basin of Kashmir Himalayas using multi-temporal satellite data. *Earth Syst Environ.* 6(2):375–389. doi: [10.1007/s41748-021-00273-y](https://doi.org/10.1007/s41748-021-00273-y).
- Ahmad ST, Ahmed R, Wani GF, Sharma P, Ahmed P. 2022b. Glacier changes in Sind basin (1990–2018) of North-western Himalayas using earth observation data. *Model Earth Syst Environ.* 8(2):2567–2579. doi: [10.1007/s40808-021-01246-w](https://doi.org/10.1007/s40808-021-01246-w).
- Ahmed R. 2024. Glacial lake outburst flood (GLOF) hazard and risk management strategies: a global overview. *Water Resour Manage.* doi: [10.1007/s11269-024-03958-x](https://doi.org/10.1007/s11269-024-03958-x).
- Ahmed R, Ahmad ST, Wani GF, Mir RA, Ahmed P, Jain SK. 2022. High resolution inventory and hazard assessment of potentially dangerous glacial Lakes in Upper Jhelum Basin, Kashmir Himalaya, India. *Geocarto Int.* 37(25), 10681–10712.
- Ahmed R., Ahmad, S. T., Wani, G. F., Mir, R. A., Almazroui, M., Bansal, J. K., & Ahmed, P. 2022a. Glacial lake changes and the identification of potentially dangerous glacial lakes (PDGLs) under warming climate in the Dibang River Basin, Eastern Himalaya, India. *Geocarto Int.* 37(27):17659–17685.
- Ahmed R, Rawat M, Wani GF, Ahmad ST, Ahmed P, Jain SK, Meraj G, Mir RA, Rather AF, Farooq M. 2022b. Glacial lake outburst flood hazard and risk assessment of Gangabal Lake in the Upper Jhelum Basin of Kashmir Himalaya using geospatial technology and hydrodynamic modeling. *Remote Sens.* 14(23):5957. doi: [10.3390/rs14235957](https://doi.org/10.3390/rs14235957).
- Ahmed, R., Wani, G. F., Ahmad, S. T., Mir, R. A., Faisal, A. A., Rather, F., & Saeed, S. (2023). Expansion of Moraine-Dammed Glacial Lakes and Historical GLOF Events in Cordillera Blanca Region of Peruvian Andes. *Earth Systems and Environment*, 7(1), 131-150. [10.1007/s41748-022-00330-0](https://doi.org/10.1007/s41748-022-00330-0)
- Allen SK, Rastner P, Arora M, Huggel C, Stoffel M. 2016. Lake outburst and debris flow disaster at Kedarnath, June 2013: hydrometeorological triggering and topographic predisposition. *Landslides.* 13(6):1479–1491. doi: [10.1007/s10346-015-0584-3](https://doi.org/10.1007/s10346-015-0584-3).
- Allen SK, Zhang G, Wang W, Yao T, Bolch T. 2019. Potentially dangerous glacial lakes across the Tibetan Plateau revealed using a large-scale automated assessment approach. *Sci Bull.* 64(7):435–445. doi: [10.1016/j.scib.2019.03.011](https://doi.org/10.1016/j.scib.2019.03.011).
- Ashraf A, Iqbal MB, Mustafa N, Naz R, Ahmad B. 2021. Prevalent risk of glacial lake outburst flood hazard in the Hindu Kush–Karakoram–Himalaya region of Pakistan. *Environ Earth Sci.* 80(12):451. doi: [10.1007/s12665-021-09740-1](https://doi.org/10.1007/s12665-021-09740-1).
- Bajracharya SR, Mool P, Shrestha BR. 2007. Impact of climate change on Himalayan glaciers and glacial lakes: case studies on GLOF and associated hazards in Nepal and Bhutan. (Vol. 12). Kathmandu: International Centre for Integrated Mountain Development.
- Banerjee P, Bhuiyan C. 2023. Glacial lakes of Sikkim Himalaya: their dynamics, trends, and likely fate—a timeseries analysis through cloud-based geocomputing, and machine learning. *Geomatics Nat Hazards Risk.* 14(1):2286903. doi: [10.1080/19475705.2023.2286903](https://doi.org/10.1080/19475705.2023.2286903).
- Barrand NE, James TD, Murray T. 2010. Spatio-temporal variability in elevation changes of two high-Arctic valley glaciers. *J Glaciol.* 56(199):771–780. doi: [10.3189/002214310794457362](https://doi.org/10.3189/002214310794457362).
- Bhambri R, Mehta M, Dobhal DP, Gupta AK, Pratap B, Kesarwani K, Verma A. 2016. Devastation in the Kedarnath (Mandakini) Valley, Garhwal Himalaya, during 16–17 June 2013: a remote sensing and ground-based assessment. *Nat Hazards.* 80(3):1801–1822. doi: [10.1007/s11069-015-2033-y](https://doi.org/10.1007/s11069-015-2033-y).
- Bhushan S, Syed TH, Arendt AA, Kulkarni AV, Sinha D. 2018. Assessing controls on mass budget and surface velocity variations of glaciers in Western Himalaya. *Sci Rep.* 8(1):8885. doi: [10.1038/s41598-018-27014-y](https://doi.org/10.1038/s41598-018-27014-y).
- Bhutiyan MR. 1999. Mass-balance studies on Siachen glacier in the Nubra valley, Karakoram Himalaya, India. *J Glaciol.* 45(149):112–118. doi: [10.3189/S0022143000003099](https://doi.org/10.3189/S0022143000003099).
- Bolch T, Buchroithner M, Pieczonka T, Kunert A. 2008. Planimetric and volumetric glacier changes in the Khumbu Himal, Nepal, since 1962 using Corona, Landsat TM and ASTER data. *J Glaciol.* 54(187):592–600. doi: [10.3189/002214308786570782](https://doi.org/10.3189/002214308786570782).

- Bolch T, Kulkarni A, Kääb A, Huggel C, Paul F, Cogley JG, Frey H, Kargel JS, Fujita K, Scheel M, et al. 2012. The state and fate of Himalayan glaciers. *Science*. 336(6079):310–314. doi: [10.1126/science.1215828](https://doi.org/10.1126/science.1215828).
- Braithwaite RJ. 2002. Glacier mass balance: the first 50 years of international monitoring. *Prog Phys Geogr*. 26(1):76–95. doi: [10.1191/0309133302pp326ra](https://doi.org/10.1191/0309133302pp326ra).
- Byers AC, Rounce DR, Shugar DH, Lala JM, Byers EA, Regmi D. 2018. A rockfall-induced glacial lake outburst flood, Upper Barun Valley, Nepal. *Landslides*. 16(3):533–549. doi: [10.1007/s10346-018-1079-9](https://doi.org/10.1007/s10346-018-1079-9).
- Che T, Xiao L, Liou YA. 2014. Changes in glaciers and glacial lakes and the identification of dangerous glacial lakes in the Pumqu River Basin, Xizang (Tibet). *Adv. Met.* 2014:1–8. doi: [10.1155/2014/903709](https://doi.org/10.1155/2014/903709).
- Clague JJ, Mathews WH. 1973. The magnitude of Jokulhlaups. *J Glaciol.* 12(66):501–504. doi: [10.3189/S0022143000031907](https://doi.org/10.3189/S0022143000031907).
- Cook SJ, Quincey DJ. 2015. Estimating the volume of Alpine glacial lakes. *Earth Surf Dynam.* 3(4):559–575. doi: [10.5194/esurf-3-559-2015](https://doi.org/10.5194/esurf-3-559-2015).
- Das S, Das S, Mandal ST, Sharma MC, Ramsankaran R. 2024. Inventory and GLOF susceptibility of glacial lakes in Chenab basin, Western Himalaya. *Geomatics Nat Hazards Risk*. 15(1):2356216. doi: [10.1080/19475705.2024.2356216](https://doi.org/10.1080/19475705.2024.2356216).
- Das S, Kar NS, Bandyopadhyay S. 2015. Glacial lake outburst flood at Kedarnath, Indian Himalaya: a study using digital elevation models and satellite images. *Nat Hazards*. 77(2): 769–786. doi: [10.1007/s11069-015-1629-6](https://doi.org/10.1007/s11069-015-1629-6).
- Ding Y, Liu J. 1992. Glacier lake outburst flood disasters in China. *Ann. Glaciol.* 16:180–184.
- Dubey S, Goyal MK. 2020. Glacial lake outburst flood hazard, downstream impact, and risk over the Indian Himalayas. *Water Resour Res.* 56(4):e2019WR026533. doi: [10.1029/2019WR026533](https://doi.org/10.1029/2019WR026533).
- Emmer A. 2018. GLOFs in the WOS: bibliometrics, geographies and global trends of research on glacial lake outburst floods (Web of Science, 1979–2016). *Nat Hazards Earth Syst Sci.* 18(3):813–827. doi: [10.5194/nhess-18-813-2018](https://doi.org/10.5194/nhess-18-813-2018).
- Emmer A, Vilímek V. 2013. Lake and breach hazard assessment for moraine-dammed lakes: an example from the Cordillera Blanca (Peru). *Nat Hazards Earth Syst Sci.* 13(6):1551–1565. doi: [10.5194/nhess-13-1551-2013](https://doi.org/10.5194/nhess-13-1551-2013).
- Emmer A, Allen SK, Carey M, Frey H, Huggel C, Korup O, Yde JC. 2022. Progress and challenges in glacial lake outburst flood research (2017–2021): a research community perspective. *Nat Hazards Earth Syst Sci Discuss.* 2022:1–34.
- Emmer A, Harrison S, Mergili M, Allen S, Frey H, Huggel C. 2020. 70 years of lake evolution and glacial lake outburst floods in the Cordillera Blanca (Peru) and implications for the future. *Geomorphology*. 365:107178. doi: [10.1016/j.geomorph.2020.107178](https://doi.org/10.1016/j.geomorph.2020.107178).
- Emmer A, Vilímek V, Zapata ML. 2018. Hazard mitigation of glacial lake outburst floods in the Cordillera Blanca (Peru): the effectiveness of remedial works. *J Flood Risk Manage.* 11(S1): s 489–S501. doi: [10.1111/jfr3.12241](https://doi.org/10.1111/jfr3.12241).
- Evans SG. 1986. The maximum discharge of outburst floods caused by the breaching of man-made and natural dams. *Can Geotech J.* 23(3):385–387. doi: [10.1139/t86-053](https://doi.org/10.1139/t86-053).
- Farinotti D, Huss M, Bauder A, Funk M. 2009. An estimate of the glacier ice volume in the Swiss Alps. *Global and Planetary Change*. 68(3):225–231. doi: [10.1016/j.gloplacha.2009.05.004](https://doi.org/10.1016/j.gloplacha.2009.05.004).
- Fujita K, Sakai A, Nuimura T, Yamaguchi S, Sharma RR. 2009. Recent changes in Imja Glacial Lake and its damming moraine in the Nepal Himalaya revealed by in situ surveys and multi-temporal ASTER imagery. *Environ Res Lett.* 4(4):045205. doi: [10.1088/1748-9326/4/4/045205](https://doi.org/10.1088/1748-9326/4/4/045205).
- Fujita K, Sakai A, Takenaka S, Nuimura T, Surazakov AB, Sawagaki T, Yamanokuchi T. 2013. Potential flood volume of Himalayan glacial lakes. *Nat Hazards Earth Syst Sci.* 13(7):1827–1839. doi: [10.5194/nhess-13-1827-2013](https://doi.org/10.5194/nhess-13-1827-2013).
- Gantayat P, Kulkarni A V, Srinivasan J. 2014. Estimation of ice thickness using surface velocities and slope: case study at Gangotri Glacier, India. *Journal of Glaciology*. 60(220):277–282. doi: [10.3189/2014JG13J078](https://doi.org/10.3189/2014JG13J078).

- Gouli MR, Hu K, Khadka N, Talchabhadel R. 2023. Hazard assessment of a pair of glacial lakes in Nepal Himalaya: unfolding combined outbursts of Upper and Lower Barun. *Geomatics Nat Hazards Risk*. 14(1):2266219. doi: [10.1080/19475705.2023.2266219](https://doi.org/10.1080/19475705.2023.2266219).
- Gupta A, Maheshwari R, Guru N, Rao BS, Raju PV, Rao VV, Sweta, (2021). Quantitative prioritization of potentially critical glacial Lakes in the Indus River basin using satellite derived parameters. *Geocarto Int*, 37(25), 7508–7530. doi: [10.1080/10106049.2021.1975831](https://doi.org/10.1080/10106049.2021.1975831).
- Haeblerli W, Schaub Y, Huggel C. 2017. Increasing risks related to landslides from degrading permafrost into new lakes in de-glaciating mountain ranges. *Geomorphology*. 293:405–417. doi: [10.1016/j.geomorph.2016.02.009](https://doi.org/10.1016/j.geomorph.2016.02.009).
- Haemmig C, Huss M, Keusen H, Hess J, Wegmüller U, Ao Z, Kulubayi W. 2014. Hazard assessment of glacial lake outburst floods from Kyagar glacier, Karakoram mountains, China. *Ann Glaciol*. 55(66):34–44. doi: [10.3189/2014AoG66A001](https://doi.org/10.3189/2014AoG66A001).
- Huggel C, Kääb A, Haeblerli W, Teyssere P, Paul F. 2002. Remote sensing-based assessment of hazards from glacier lake outbursts: a case study in the Swiss Alps. *Can Geotech J*. 39(2): 316–330. doi: [10.1139/t01-099](https://doi.org/10.1139/t01-099).
- Hussain A, Nasab N, Bano D, Karim D, Anwar W, Hussain K, Uddin N. 2020. Glacier lake outburst flood modeling of Khurdopin glacier lake using HEC-RAS and GIS. In: *Селевые потоки: катастрофы, риск, прогноз, защита*. p. 208–220.
- Ikeda N, Narama C, Gyalsen S. 2016. Knowledge sharing for disaster risk reduction: insights from a glacier lake workshop in the Ladakh region, Indian Himalayas. *Mt Res Dev*. 36(1): 31–40. doi: [10.1659/MRD-JOURNAL-D-15-00035.1](https://doi.org/10.1659/MRD-JOURNAL-D-15-00035.1).
- Imdad K, Rihan M, Sahana M, Parween S, Ahmed R, Costache R, Chaudhary A, Tripathi R. 2023. Wetland health, water quality, and resident perceptions of declining ecosystem services: a case study of Mount Abu, Rajasthan, India. *Environ Sci Pollut Res Int*. 30(55): 116617–116643. doi: [10.1007/s11356-022-21902-7](https://doi.org/10.1007/s11356-022-21902-7).
- Ives JD, Shrestha RB, Mool PK. 2010. Formation of glacial lakes in the Hindu Kush Himalayas and GLOF risk assessment. Kathmandu: International Centre for Integrated Mountain Development; p. 10–11.
- Jiang S, Nie Y, Liu Q, Wang J, Liu L, Hassan J, Liu X, Xu X. 2018. Glacier change, supraglacial debris expansion and glacial lake evolution in the Gyirong River Basin, Central Himalayas, between 1988 and 2015. *Remote Sens*. 10(7):986. doi: [10.3390/rs10070986](https://doi.org/10.3390/rs10070986).
- Kaplan G, Avdan U. 2017. Object-based water body extraction model using Sentinel-2 satellite imagery. *Eur J Remote Sens*. 50(1):137–143. doi: [10.1080/22797254.2017.1297540](https://doi.org/10.1080/22797254.2017.1297540).
- Kargel JS, Leonard GJ, Shugar DH, Haritashya UK, Bevington A, Fielding EJ, Fujita K, Geertsema M, Miles ES, Steiner J, et al. 2016. Geomorphic and geologic controls of geohazards induced by Nepal's 2015 Gorkha earthquake. *Science*. 351(6269):aac8353. doi: [10.1126/science.aac8353](https://doi.org/10.1126/science.aac8353).
- Khadka N, Chen, X., Nie, Y., Thakuri, S., Zheng, G., & Zhang, G. 2021. Evaluation of Glacial Lake Outburst Flood susceptibility using multi criteria assessment framework in Mahalangur Himalaya. *Front Earth Sci*. 8:601288.
- Klimeš J, Benešová M, Vilímek V, Bouška P, Cochachin Rapre A. 2014. The reconstruction of a glacial lake outburst flood using HEC-RAS and its significance for future hazard assessments: an example from Lake 513 in the Cordillera Blanca, Peru. *Nat Hazards*. 71(3):1617–1638. doi: [10.1007/s11069-013-0968-4](https://doi.org/10.1007/s11069-013-0968-4).
- Kulkarni AV. 1992. Mass balance of Himalayan glaciers using AAR and ELA methods. *J Glaciol*. 38(128):101–104. doi: [10.3189/S0022143000009631](https://doi.org/10.3189/S0022143000009631).
- Kumar A, Negi HS, Kumar K, Shekhar C, Kanda N. 2019. Quantifying mass balance of East-Karakoram glaciers using geodetic technique. *Polar Sci*. 19:24–39. doi: [10.1016/j.polar.2018.11.005](https://doi.org/10.1016/j.polar.2018.11.005).
- Liu Q, Mayer C, Wang X, Nie Y, Wu K, Wei J, Liu S. 2020. Interannual flow dynamics driven by frontal retreat of a lake-terminating glacier in the Chinese Central Himalaya. *Earth and Planetary Science Letters*. 546:116450. doi: [10.1016/j.epsl.2020.116450](https://doi.org/10.1016/j.epsl.2020.116450).

- Kumar GV, Kulkarni AV, Gupta AK, Sharma P. 2017. Mass balance estimation using geodetic method for glaciers in Baspa basin, Western Himalaya. *Curr Sci.* 113(03):486–492. doi: [10.18520/cs/v113/i03/486-492](https://doi.org/10.18520/cs/v113/i03/486-492).
- Majeed U, Rashid I, Najar NA, Gul N. 2021. Spatiotemporal dynamics and geodetic mass changes of glaciers with varying debris cover in the Pangong region of Trans-Himalayan Ladakh, India between 1990 and 2019. *Front Earth Sci.* 9:748107. doi: [10.3389/feart.2021.748107](https://doi.org/10.3389/feart.2021.748107).
- Majeed U, Rashid I, Sattar A, Allen S, Stoffel M, Nüsser M, Schmidt S. 2021. Recession of Gya Glacier and the 2014 glacial lake outburst flood in the trans-Himalayan region of Ladakh, India. *Sci Total Environ.* 756:144008. doi: [10.1016/j.scitotenv.2020.144008](https://doi.org/10.1016/j.scitotenv.2020.144008).
- Mal S, Allen SK, Frey H, Huggel C, Dimri AP. 2021. Sectorwise assessment of glacial lake outburst flood danger in the Indian Himalayan region. *Mt Res Dev.* 41(1):R1. doi: [10.1659/MRD-JOURNAL-D-20-00043.1](https://doi.org/10.1659/MRD-JOURNAL-D-20-00043.1).
- Malik IH, Ahmed R, Ford JD, Shakoor MSA, Wani SN. 2024. Beyond the banks and deluge: understanding riverscape, flood vulnerability, and responses in Kashmir. *Nat Hazards.* doi: [10.1007/s11069-024-06712-z](https://doi.org/10.1007/s11069-024-06712-z).
- Mann R, Gupta A, Sharma S, Saini D, Koul MN, Mann R. 2022. Time-series trend analysis of precipitation and temperature over Ladakh, India.
- McFeeters SK. 1996. The use of the normalized difference water index (NDWI) in the delineation of open water features. *Int J Remote Sens.* 17(7):1425–1432. doi: [10.1080/01431169608948714](https://doi.org/10.1080/01431169608948714).
- Mir RA, Jain SK, Lohani AK, Ahmed R, Ahmad ST, Wani GF. 2022. Application of mike 11 for one-dimensional GLOF modeling of a rapidly expanding Dalung Proglacial Lake, Indus River Basin, Western Himalaya. In: *Challenges of disasters in Asia: vulnerability, adaptation and resilience*. Singapore: Springer Nature Singapore; p. 147–161.
- Mir RA, Jain SK, Lohani AK, Saraf AK. 2018. Glacier recession and glacial lake outburst flood studies in Zaskar basin, western Himalaya. *J. Hydrol.* 564:376–396. doi: [10.1016/j.jhydrol.2018.05.031](https://doi.org/10.1016/j.jhydrol.2018.05.031).
- Mool PK. 1995. Glacier lake outburst floods in Nepal. *J Nepal Geol Soc.* 11(1995):173–280. doi: [10.3126/jngs.v11i0.32802](https://doi.org/10.3126/jngs.v11i0.32802).
- Muhammad S, Tian L, Khan A. 2019. Early twenty-first century glacier mass losses in the Indus Basin constrained by density assumptions. *J Hydrol.* 574:467–475. doi: [10.1016/j.jhydrol.2019.04.057](https://doi.org/10.1016/j.jhydrol.2019.04.057).
- Mushtaq S, Saleem S, Ahmed R, Tass MS, Rather JA, Rather GM. 2024. Spatio-temporal analysis land use land cover changes in South Kashmir region of North-western Himalayas using Landsat data. *Discov Geosci.* 2(1):37. doi: [10.1007/s44288-024-00031-3](https://doi.org/10.1007/s44288-024-00031-3).
- Narama C, Daiyrov M, Duishonakunov M, Tadono T, Sato H, Kääb A, Ukita J, Abdrakhmatov K. 2018. Large drainages from short-lived glacial lakes in the Teskey Range, Tien Shan Mountains, Central Asia. *Nat Hazards Earth Syst Sci.* 18(4):983–995. doi: [10.5194/nhess-18-983-2018](https://doi.org/10.5194/nhess-18-983-2018).
- Nie Y, Liu Q, Wang J, Zhang Y, Sheng Y, Liu S. 2018. An inventory of historical glacial lake outburst floods in the Himalayas based on remote sensing observations and geomorphological analysis. *Geomorphology.* 308:91–106. doi: [10.1016/j.geomorph.2018.02.002](https://doi.org/10.1016/j.geomorph.2018.02.002).
- Nie Y, Sheng Y, Liu Q, Liu L, Liu S, Zhang Y, Song C. 2017. A regional-scale assessment of Himalayan glacial lake changes using satellite observations from 1990 to 2015. *Remote Sens. Environ.* 189:1–13. doi: [10.1016/j.rse.2016.11.008](https://doi.org/10.1016/j.rse.2016.11.008).
- Patel LK, Sharma P, Laluraj CM, Thamban M, Singh A, Ravindra R. 2017. A geospatial analysis of Samudra Tapu and Gepang Gath glacial lakes in the Chandra Basin, Western Himalaya. *Nat Hazards.* 86(3):1275–1290. doi: [10.1007/s11069-017-2743-4](https://doi.org/10.1007/s11069-017-2743-4).
- Paterson WSB. 1991. Why ice-age ice is sometimes “soft. *Cold Reg. Sci. Technol.* 20(1):75–98. doi: [10.1016/0165-232X\(91\)90058-O](https://doi.org/10.1016/0165-232X(91)90058-O).
- Paul F, Bolch T, Kääb A, Nagler T, Nuth C, Scharrer K, Van Niel T. 2015. The glaciers climate change initiative: Methods for creating glacier area, elevation change and velocity products. *Remote Sensing of Environment.* 162:408–426. doi: [10.1016/j.rse.2013.07.043](https://doi.org/10.1016/j.rse.2013.07.043).

- Petrakov DA, Chernomorets SS, Viskhadzhieva KS, Dokukin MD, Savernyuk EA, Petrov MA, Erokhin SA, Tutubalina OV, Glazyrin GE, Shpuntova AM, et al. 2020. Putting the poorly documented 1998 GLOF disaster in Shakhimardan River valley (Alay Range, Kyrgyzstan/Uzbekistan) into perspective. *Sci Total Environ.* 724:138287. doi: [10.1016/j.scitotenv.2020.138287](https://doi.org/10.1016/j.scitotenv.2020.138287).
- Pratap B, Dobhal DP, Bhambri R, Mehta M, Tewari VC. 2016. Four decades of glacier mass balance observations in the Indian Himalaya. *Reg Environ Change.* 16(3):643–658. doi: [10.1007/s10113-015-0791-4](https://doi.org/10.1007/s10113-015-0791-4).
- Qi M, Liu S, Wu K, Zhu Y, Xie F, Jin H, Gao Y, Yao X. 2022. Improving the accuracy of glacial lake volume estimation: a case study in the Poiqu basin, central Himalayas. *J Hydrol.* 610:127973. doi: [10.1016/j.jhydrol.2022.127973](https://doi.org/10.1016/j.jhydrol.2022.127973).
- Raj KBG, Remya SN, Kumar KV. 2013. Remote sensing-based hazard assessment of glacial lakes in Sikkim Himalaya. *Curr Sci.* 359–364.
- Rashid I, Majeed U, Jan A, Glasser NF. 2020. The January 2018 to September 2019 surge of Shisper Glacier, Pakistan, detected from remote sensing observations. *Geomorphology.* 351:106957 [10.1016/j.geomorph.2019.106957](https://doi.org/10.1016/j.geomorph.2019.106957).
- Rather AF, Ahmed R, Ahmed P, Bansal JK, Banerjee P, Wani TA, Javaid S, Mir RA. 2024b. Examining the glacier-glacial lake interactions of potentially dangerous glacial lakes (PDGLs) under changing climate in Shyok catchment of the Upper Indus Basin. *Phys Chem Earth A/B/C.* 136:103686. doi: [10.1016/j.pce.2024.103686](https://doi.org/10.1016/j.pce.2024.103686).
- Rather AF, Ahmed R, Jun C, Bateni SM, Ahmed P, Mir RA. 2024a. Understanding glacial lake evolution and the associated GLOF hazard in the Shyok catchment of the Upper Indus Basin using geospatial techniques. *Nat Hazards Rev.* 25(3):04024014. doi: [10.1061/NHREFO.NHENG-1988](https://doi.org/10.1061/NHREFO.NHENG-1988).
- Rawat M, Ahmed R, Jain SK, Lohani AK, Rongali G, Tiwari KC. 2023a. Glacier–glacial lake changes and modeling glacial lake outburst flood in Upper Ganga Basin, India. *Model Earth Syst Environ.* 9(1):507–526. doi: [10.1007/s40808-022-01512-5](https://doi.org/10.1007/s40808-022-01512-5).
- Rawat M, Jain SK, Ahmed R, Lohani AK. 2023b. Glacial lake outburst flood risk assessment using remote sensing and hydrodynamic modeling: a case study of Satluj basin, Western Himalayas, India. *Environ Sci Pollut Res Int.* 30(14):41591–41608. doi: [10.1007/s11356-023-25134-1](https://doi.org/10.1007/s11356-023-25134-1).
- Reynolds JM. 1998. High-altitude glacial lake hazard assessment and mitigation: a Himalayan perspective. *EGSP.* 15(1):25–34. doi: [10.1144/GSL.ENG.1998.015.01.03](https://doi.org/10.1144/GSL.ENG.1998.015.01.03).
- Richardson SD, Reynolds JM. 2000. An overview of glacial hazards in the Himalayas. *Quat. Int.* 65–66(1):31–47. doi: [10.1016/S1040-6182\(99\)00035-X](https://doi.org/10.1016/S1040-6182(99)00035-X).
- Romshoo S A, Abdullah T, Murtaza K O, Bhat M H. 2023. Direct, geodetic and simulated mass balance studies of the Kolahoi Glacier in the Kashmir Himalaya, India. *Journal of Hydrology.* 617:129019 [10.1016/j.jhydrol.2022.129019](https://doi.org/10.1016/j.jhydrol.2022.129019).
- Rounce DR, Watson CS, McKinney DC. 2017. Identification of hazard and risk for glacial lakes in the Nepal Himalaya using satellite imagery from 2000–2015. *Remote Sens.* 9(7):654. doi: [10.3390/rs9070654](https://doi.org/10.3390/rs9070654).
- Round V, Leinss S, Huss M, Haemmig C, Hajnsek I. 2017. Surge dynamics and lake outbursts of Kyagar Glacier, Karakoram. *Cryosphere.* 11(2):723–739. doi: [10.5194/tc-11-723-2017](https://doi.org/10.5194/tc-11-723-2017).
- Saleem H, Ahmed R, Mushtaq S, Saleem S, Rajesh M. 2024. Remote sensing-based analysis of land use, land cover, and land surface temperature changes in Jammu District, India. *Int J River Basin Manag.* 1–16. doi: [10.1080/15715124.2024.2327493](https://doi.org/10.1080/15715124.2024.2327493).
- Sattar A, Goswami A, Kulkarni AV. 2019. Application of 1D and 2D hydrodynamic modeling to study glacial lake outburst flood (GLOF) and its impact on a hydropower station in Central Himalaya. *Nat Hazards.* 97(2):535–553. doi: [10.1007/s11069-019-03657-6](https://doi.org/10.1007/s11069-019-03657-6).
- Sattar A, Goswami A, Kulkarni AV. 2019. Hydrodynamic moraine-breach modeling and outburst flood routing-A hazard assessment of the South Lhonak lake, Sikkim. *Sci Total Environ.* 668:362–378. doi: [10.1016/j.scitotenv.2019.02.388](https://doi.org/10.1016/j.scitotenv.2019.02.388).

- Sattar A, Haritashya UK, Kargel JS, Leonard GJ, Shugar DH, Chase DV. 2021. Modeling lake outburst and downstream hazard assessment of the Lower Barun Glacial Lake, Nepal Himalaya. *J Hydrol.* 598:126208. doi: [10.1016/j.jhydrol.2021.126208](https://doi.org/10.1016/j.jhydrol.2021.126208).
- Schaub Y, Huggel C, Cochachin A. 2016. Ice-avalanche scenario elaboration and uncertainty propagation in numerical simulation of rock-/ice-avalanche-induced impact waves at Mount Hualcán and Lake 513, Peru. *Landslides.* 13(6):1445–1459. doi: [10.1007/s10346-015-0658-2](https://doi.org/10.1007/s10346-015-0658-2).
- Schmidt S, Nüsser M, Baghel R, Dame J. 2020. Cryosphere hazards in Ladakh: the 2014 Gya glacial lake outburst flood and its implications for risk assessment. *Nat Hazards.* 104(3): 2071–2095. doi: [10.1007/s11069-020-04262-8](https://doi.org/10.1007/s11069-020-04262-8).
- Shafiq MU, Bhat MS, Rasool R, Ahmed P, Singh H, Hassan H. 2016. Variability of precipitation regime in Ladakh region of India from 1901–2000. *JCWF.* 4(2):165.
- Shrestha AB, Eriksson M, Mool P, Ghimire P, Mishra B, Khanal NR. 2010. Glacial lake outburst flood risk assessment of Sun Koshi basin, Nepal. *Geomatics Nat Hazards Risk.* 1(2): 157–169. doi: [10.1080/19475701003668968](https://doi.org/10.1080/19475701003668968).
- Sorucu A, Vincent C, Francou B, Ribstein P, Berger T, Sicart JE, Wagnon P, Arnaud Y, Favier V, Lejeune Y. 2009. Mass balance of Glacier Zongo, Bolivia, between 1956 and 2006, using glaciological, hydrological and geodetic methods. *Ann Glaciol.* 50(50):1–8. doi: [10.3189/172756409787769799](https://doi.org/10.3189/172756409787769799).
- Taylor C, Robinson TR, Dunning S, Rachel Carr J, Westoby M. 2023. Glacial lake outburst floods threaten millions globally. *Nat Commun.* 14(1):487. doi: [10.1038/s41467-023-36033-x](https://doi.org/10.1038/s41467-023-36033-x).
- Wang W, Gao Y, Iribarren Anaconda P, Lei Y, Xiang Y, Zhang G, Li S, Lu A. 2018. Integrated hazard assessment of Cirenmaco glacial lake in Zhangzangbo valley, Central Himalayas. *Geomorphology.* 306:292–305. doi: [10.1016/j.geomorph.2015.08.013](https://doi.org/10.1016/j.geomorph.2015.08.013).
- Wang W, Yao T, Gao Y, Yang X, Kattel DB. 2011. A first-order method to identify potentially dangerous glacial lakes in a region of the southeastern Tibetan Plateau. *Mt Res Dev.* 31(2): 122–130. doi: [10.1659/MRD-JOURNAL-D-10-00059.1](https://doi.org/10.1659/MRD-JOURNAL-D-10-00059.1).
- Wang W, Zhang T, Yao T, An B. 2022. Monitoring and early warning system of Cirenmaco glacial lake in the central Himalayas. *Int J Disaster Risk Reduct.* 73:102914. doi: [10.1016/j.ijdrr.2022.102914](https://doi.org/10.1016/j.ijdrr.2022.102914).
- Wang X, Guo X, Yang C, Liu Q, Wei J, Zhang Y, Liu S, Zhang Y, Jiang Z, Tang Z. 2020. Glacial lake inventory of high-mountain Asia in 1990 and 2018 derived from Landsat images. *Earth Syst Sci Data.* 12(3):2169–2182. doi: [10.5194/essd-12-2169-2020](https://doi.org/10.5194/essd-12-2169-2020).
- Worni R, Huggel C, Stoffel M. 2013. Glacial lakes in the Indian Himalayas – From an area-860 wide glacial lake inventory to on-site and modeling-based risk assessment of critical glacial 861 lakes. *Sci Total Environ.* 468-469 Suppl:S71–S84. doi: [10.1016/j.scitotenv.2012.11.043](https://doi.org/10.1016/j.scitotenv.2012.11.043).
- Worni R, Huggel C, Clague JJ, Schaub Y, Stoffel M. 2014. Coupling glacial lake impact, dam breach, and flood processes: a modeling perspective. *Geomorphology.* 224:161–176. doi: [10.1016/j.geomorph.2014.06.031](https://doi.org/10.1016/j.geomorph.2014.06.031).
- Zemp M, Hoelzle M, Haeblerli W. 2009. Six decades of glacier mass-balance observations: a review of the worldwide monitoring network. *Ann Glaciol.* 50(50):101–111., doi: [10.3189/172756409787769591](https://doi.org/10.3189/172756409787769591).
- Zhang G, Carrivick JL, Emmer A, Shugar DH, Veh G, Wang X, Labedz C, Mergili M, Mölg N, Huss M, et al. 2024. Characteristics and changes of glacial lakes and outburst floods. *Nat Rev Earth Environ.* 5(6):447–462. doi: [10.1038/s43017-024-00554-w](https://doi.org/10.1038/s43017-024-00554-w).
- Zhang M, Chen F, Guo H, Yi L, Zeng J, Li B. 2022. Glacial Lake area changes in high mountain asia during 1990–2020 using satellite remote sensing. *Research.* 2022:9821275. doi: [10.34133/2022/9821275](https://doi.org/10.34133/2022/9821275).
- Zhang M, Chen F, Tian B, Liang D, Yang A. 2020. Characterization of Kyagar Glacier and lake outburst floods in 2018 based on time-series Sentinel-1A data. *Water.* 12(1):184. doi: [10.3390/w12010184](https://doi.org/10.3390/w12010184).